Plant Mol Biol (2011) 75:141–165
DOI 10.1007/s11103-010-9715-3

Differences in gene expression amplitude overlie a conserved transcriptomic program occurring between the rapid and potent localized resistant reaction at the syncytium of the *Glycine max* genotype Peking (PI 548402) as compared to the prolonged and potent resistant reaction of PI 88788

Vincent P. Klink · Parsa Hosseini · Prachi D. Matsye · Nadim W. Alkharouf · Benjamin F. Matthews

Received: 2 October 2009 / Accepted: 13 November 2010 / Published online: 14 December 2010

Abstract *Glycine max* L. Merr. (soybean) resistance to *Heterodera glycines* Ichinohe occurs at the site of infection, a nurse cell known as the syncytium. Resistance is classified into two cytologically-defined responses, the *G. max*$_{[Peking]}$- and *G. max*$_{[PI\ 88788]}$-types. Each type represents a cohort of *G. max* genotypes. Resistance in *G. max*$_{[Peking]}$ occurs by a potent and rapid localized response, affecting parasitic second stage juveniles (p-J2). In contrast, resistance occurs by a potent but more prolonged reaction in the genotype *G. max*$_{[PI\ 88788]}$ that affects nematode development at the J3 and J4 stages. Microarray analyses comparing these cytologically and developmentally distinct resistant reactions reveal differences in gene expression in pericycle and surrounding cells even before infection. The differences include higher relative levels of the differentially expressed in response to arachidonic acid 1 gene (*DEA1* [*Gm*-DEA1]) (+224.19-fold) and a protease inhibitor (+68.28-fold) in *G. max*$_{[Peking/PI\ 548402]}$ as compared to *G. max*$_{[PI\ 88788]}$. Gene pathway analyses compare the two genotypes (1) before, (2) at various times during, (3) constitutively throughout the resistant reaction and (4) at all time points prior to and during the resistant reaction. The amplified levels of transcriptional activity of defense genes may explain the rapid and potent reaction in *G. max*$_{[Peking/PI\ 548402]}$ as compared to *G. max*$_{[PI\ 88788]}$. In contrast, the shared differential expression levels of genes in *G. max*$_{[Peking/PI\ 548402]}$ and *G. max*$_{[PI\ 88788]}$ may indicate a conserved genomic program underlying the *G. max* resistance on which the genotype-specific gene expression programs are built off.

Keywords Soybean · *Glycine max* · Soybean cyst nematode · SCN · *Heterodera glycines* · Microarray · Gene expression · Plant pathogen · Parasite · Affymetrix® · Laser capture microdissection · PI 88788 · Peking · PI 548402 · Transcriptome, genome, gene expression, value

Abbreviations

EST	Expressed sequence tag
hpi	Hours post inoculation
dpi	Days post inoculation
SCN	Soybean cyst nematode
J2	Second stage juvenile
FS	Farmer's solution
LCM	Laser capture microdissection

Introduction

The infection of plants by parasitic nematodes is a major, ubiquitous, dominant and persistent problem for

Electronic supplementary material The online version of this article (doi:10.1007/s11103-010-9715-3) contains supplementary material, which is available to authorized users.

V. P. Klink (✉) · P. D. Matsye
Department of Biological Sciences, Harned Hall, Mississippi State University, Mississippi State, MS 39762, USA
e-mail: vklink@biology.msstate.edu

P. Hosseini · B. F. Matthews
United States Department of Agriculture, Soybean Genomics and Improvement Laboratory, Bldg. 006, Beltsville, MD 20705, USA

P. Hosseini · N. W. Alkharouf
Jess and Mildred Fisher College of Science and Mathematics, Department of Computer and Information Sciences, Towson University, 7800 York Road, Towson, MD 21252, USA

agriculture, worldwide. Estimates rate worldwide agronomic losses to plant parasitic nematodes at 100–157 billion dollars, annually (Sasser and Freckman 1987; Abad et al. 2008). However, the ability to resist infection exists in the germplasm of many agricultural plants, including one of the most important, soybean (*Glycine max*). The dominant pathogen of *G. max* is the parasitic nematode *Heterodera glycines* (soybean cyst nematode; Wrather et al. 2001; Wrather and Koenning 2006). Many natural collections of *G. max* have been made, providing a bank of accessions (genotypes) that are catalogued by a plant introduction (PI) number. The numerous *G. max* accessions have been tested for their ability to resist infection by *H. glycines* (reviewed in Riggs 1992; reviewed in Shannon et al. 2004). From those studies, two major cohorts of PIs, each composed of a few *G. max* genotypes, were shown to exhibit specific but contrasting ways to combat *H. glycines* at the site of infection, a nurse cell known as a syncytium. The cohorts are each defined by their respective agronomically important archetypes, *G. max* Peking (*G. max*$_{[Peking]}$) and *G. max* PI 88788 (*G. max*$_{[PI\ 88788]}$). Importantly, *G. max*$_{[Peking]}$ and *G. max*$_{[PI\ 88788]}$ are the sources of greater than 95% of the resistance germplasm that is bred into commercial varieties (reviewed in Concibido et al. 2004). The response of *G. max*$_{[Peking]}$ to *H. glycines* infection is characterized by a potent and rapid resistance reaction (Klink et al. 2009a). It is potent because, depending on the *H. glycines* population infecting *G. max*, the nematodes die at the parasitic second stage juvenile (p-J2). In contrast, *G. max*$_{[PI\ 88788]}$ is characterized by a potent but prolonged resistant reaction (Klink et al. 2010a) where nematodes die at the J3 and J4 stages. An interesting feature of these resistant reactions, occurring at the syncytium, is that their underlying cytology is very different. While only a few molecular investigations have studied those contrasting forms of the resistant reaction (Klink et al. 2007a, b, 2009a, 2010a, b), they have never been directly compared to each other until now. Thus, it has not been determined how a single nematode population can elicit the development of two completely different resistant reactions at the site of infection. In the studies presented here, the *H. glycines* population, HG-type 7, was used to infect both the *G. max*$_{[PI\ 548402]}$ genetic background of the genotype Peking (*G. max*$_{[Peking/PI\ 548402]}$) and *G. max*$_{[PI\ 88788]}$. The experiments determined the gene expression pattern as a single pure nematode population elicits two completely different cellular responses culminating in resistant reactions in *G. max*$_{[Peking/PI\ 548402]}$ and *G. max*$_{[PI\ 88788]}$.

What makes these experiments important is that very few studies in agriculturally important plant systems have identified genes that relate to or confer resistance to parasitic nematodes. For example, Cai et al. (1997) identified a resistance (R) gene in *Beta procumbens* (sugar beet) that yields an incompatible reaction to the beet cyst nematode *Heterodera schachtii*. Milligan et al. (1998) identified the R gene, *Mi*, in *Lycopersicon esculentum* (tomato) to the giant cell-forming plant parasitic nematode *Meloidiogyne incognita*. The *Mi* gene has been shown to encode a leucine rich repeat (LRR) protein, a family of proteins with a long history of being involved in plant defense (Jones et al. 1994). Other genes that are involved in the resistance process to plant parasitic nematodes have also been identified. For example, Gao et al. (2008) identified the 9-lipoxygenase (ZmLOX-3) gene of *Zea mays* (corn), responsible for resistance to *M. incognita*. The work of Gao et al. (2008) implicates jasmonic acid signaling and lipid metabolism in defense to plant parasitic nematodes. LOX is the most highly induced gene, locally within syncytia undergoing an incompatible reaction as compared to the syncytia undergoing a compatible reaction in *G. max* (Klink et al. 2007a, 2009a). Other genes of the LOX signaling pathway have also been shown to be induced (Klink et al. 2009a, 2010a).

The identification of the nematode resistance genes in important agricultural plants such as *G. max* would greatly help efforts to improving their value. *Glycine max* currently is the top rated export crop in the US and the source of 70% (157 million metric tons) of the world's protein meal. Decades of gene mapping studies have been done to identify those resistance loci in *G. max* (reviewed in Concibido et al. 2004). The genetic mapping investigations reveal the resistance of *G. max* to *H. glycines* is multigenic, composed of both recessive and dominant genes (reviewed in Concibido et al. 2004). The recessive genes are *rhg1*, *rhg2* and *rhg3* (Caldwell et al. 1960). The two dominant resistance genes are *Rhg4* (Matson and Williams 1965) and *Rhg5* (Rao-Arelli 1994).

As mentioned previously, *G. max*$_{[Peking]}$ and *G. max*$_{[PI\ 88788]}$ are the archetypal sources of almost all the germplasm that is bred into commercial varieties of soybean. The underlying nature of *G. max*$_{[Peking]}$ resistance is *rhg1*, *rhg2*, and *rhg3*, accompanied by the dominant gene *Rhg4* (Matson and Williams 1965). The *G. max*$_{[PI\ 88788]}$ resistance is explained by *rhg1*, *rhg2*, *Rhg4* and *Rhg5* (Glover et al. 2004; reviewed in Concibido et al. 2004). Those studies document that both *G. max*$_{[Peking]}$ and *G. max*$_{[PI\ 88788]}$ harbor *rhg1*, *rhg2*, and *Rhg5* while *G. max*$_{[Peking]}$ has *rhg3* and *G. max*$_{[PI\ 88788]}$ has *Rhg5*. Other less well understood resistance factors have been identified through quantitative trait loci (QTL) mapping studies in *G. max*$_{[Peking]}$ and *G. max*$_{[PI\ 88788]}$ (reviewed in Concibido et al. 2004).

Understanding the nature of the resistance genes is not a straightforward process. The complication comes from the number of field isolated populations of *H. glycines* that

have varying capacities to infect the numerous *G. max* genotypes (Ross 1962). Currently, there are 16 historically accepted *H. glycines* races (Riggs and Schmitt 1988, 1991; Riggs 1988). However, more recent research has resulted in a reclassification of *H. glycines* races as distinct populations because they can only be maintained through a sexual reproductive cycle (Niblack et al. 2002). The reclassification scheme was made possible because more *G. max* genotypes that exhibit various levels of resistance are available and more sophisticated tests have been developed over the years that could tease out the fine details of the infective capability of unknown *H. glycines* populations (Niblack et al. 2002). The identity of an unknown field isolated population is determined by an *H. glycines* type (HG-type) test. During the HG-type test, the nematode is allowed to infect a known susceptible genotype along with a panel of seven or more *G. max* genotypes with varying abilities to resist infection by the different *H. glycines* populations (Niblack et al. 2002). The HG-type test is based off of other studies (Ross 1962; Golden et al. 1970; Riggs and Schmitt 1988, 1991; Riggs 1988). Thus, the revised HG-type test is an important development in *H. glycines* research. However, the HG-type test does not provide information on how various *G. max* genotypes accomplish resistance at the site of infection (i.e., the syncytium). Such information would provide useful knowledge in understanding how each resistant *G. max* genotype alters their gene expression to accomplish resistance.

The resistant reaction at the syncytium undergoes two distinct developmental phases that have been documented at the cytological and ultrastructural levels (Endo 1965, 1991; Riggs et al. 1973; Acido et al. 1984; Kim et al. 1987; Halbrendt et al. 1992; Kim and Riggs 1992; Mahalingham and Skorupska 1996; Klink et al. 2007a, b, 2009a, 2010a, b). The first phase (phase 1) occurs when the nematode appears to be engaging the parasitism machinery to initiate the formation of the syncytium. During phase 1, the syncytium of both resistant and susceptible reactions appears the same (Endo 1965; Riggs et al. 1973; Acido et al. 1984; Kim et al. 1987). Phase 1 includes the dissolution of cell walls, enlargement of nuclei, limited hypertrophy, the presence of dense cytoplasm and increased ER content (Endo 1965; Riggs et al. 1973; Kim et al. 1987). Phase 1 occurs between 1 and 4 days post inoculation (dpi), depending on the genotype of *G. max* (Endo 1965; Riggs et al. 1973; Kim et al. 1987). The second phase (phase 2) of the resistance reaction becomes evident at both the cytological and ultrastructural levels by 4–5 dpi (Endo 1965; Riggs et al. 1973; Acido et al. 1984; Kim et al. 1987). The resistance characteristics are dependent on the genotype of *G. max*.

A rudimentary classification scheme of *G. max* resistance has been developed from the cytological, ultrastructural and developmental comparative analyses of how the various *G. max* genotypes react to *H. glycines* (Colgrove and Niblack 2008). The work has resulted in the designation of the *G. max*$_{[\text{Peking}]}$ and *G. max*$_{[\text{PI 88788}]}$ groups (Colgrove and Niblack 2008; Fig. 1). The designation of the *G. max*$_{[\text{Peking}]}$ and *G. max*$_{[\text{PI 88788}]}$ groups are based on numerous observations (Ross 1958; Endo 1965; Riggs et al. 1973; Acido et al. 1984; Kim et al. 1987; Halbrendt et al. 1992; Kim and Riggs 1992; Mahalingham and Skorupska 1996). The *G. max*$_{[\text{Peking}]}$ group includes the

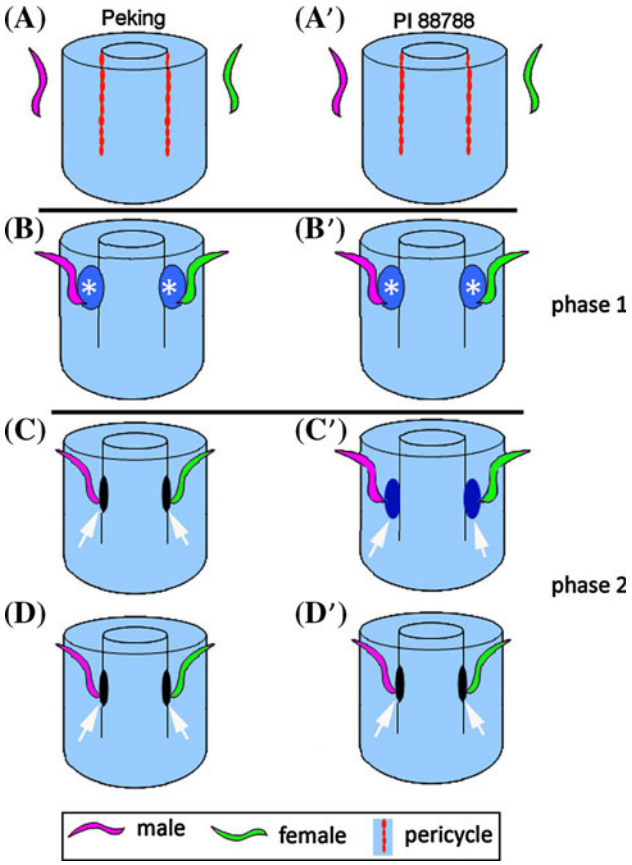

Fig. 1 *G. max*$_{[\text{Peking/PI 548402}]}$ and *G. max*$_{[\text{PI 88788}]}$ resistant reactions. **a**,**a**′ Male (*magenta*) and female (*green*) pre-infective J2 (pi-J2) nematodes migrate toward the root. **b**,**b**′ The infective J2 (i-J2) nematodes burrow into the root and migrate toward the root stele, typically selecting a pericycle or neighboring cell as the feeding site initial (FS_i) and create a syncytium (*white asterisk*). The earlier stages of syncytium development (between 1 an 4 dpi) are similar between *G. max*$_{[\text{Peking}]}$ and *G. max*$_{[\text{PI 88788}]}$-type of resistant reactions. **c** In the *G. max*$_{[\text{Peking}]}$-type, a rapid and potent resistant reaction occurs by the formation of a necrotic region that surrounds the syncytium (*black oval*, *white arrow*) by 4 dpi. **c**′ In the *G. max*$_{[\text{PI 88788}]}$-type of resistance reaction, a slower response, characterized initially by nuclear degeneration within the syncytium (*dark blue oval*, *white arrow*), occurs by 5 dpi. **d** The *G. max*$_{[\text{Peking}]}$-type of resistant reaction is characterized by the later stages of syncytium degeneration (*black oval*, *white arrow*) at 7 dpi. **d**′ The *G. max*$_{[\text{PI 88788}]}$-type of resistant reaction is characterized by the later stages of syncytium degeneration as the cytoplasm degrades (*black oval*, *white arrow*) at 10 dpi. (Timing of stages adapted from Endo 1965; Riggs et al. 1973; Lauritis et al. 1983; Kim et al. 1987.)

genotypes *G. max*$_{[Peking]}$, *G. max*$_{[PI\ 90763]}$, *G. max*$_{[PI\ 89772]}$ and partially *G. max*$_{[PI\ 437654]}$. The *G. max*$_{[PI\ 88788]}$ group includes *G. max*$_{[PI\ 88788]}$, *G. max*$_{[PI\ 209332]}$ and *G. max*$_{[PI\ 548316]}$ (Colgrove and Niblack 2008). In addition to documenting the cellular reaction of the syncytium as it degenerates as a consequence of its interaction with the nematode, the work has also documented the differences in stages when nematode development arrests during the *G. max*$_{[Peking]}$ and *G. max*$_{[PI\ 88788]}$-types of resistant reactions.

Cytological work has documented that there is an earlier response to nematode infection during the *G. max*$_{[Peking]}$-type of resistant reaction (Endo 1965; Riggs et al. 1973; Acido et al. 1984; Kim et al. 1987; Kim and Riggs 1992). Cytological observations reveal that the *G. max*$_{[Peking]}$-type of resistance response involves necrosis of the syncytial cells that surround the head of the nematode. The necrotic layer separates the syncytium from the surrounding cells (Kim et al. 1987). The resistant reaction in the *G. max*$_{[Peking]}$ archetype has a characteristic cytology that accompanies these cytological features. The *G. max*$_{[Peking]}$ resistant reaction includes the formation of cell wall appositions (CWA). The CWAs are structures defined as physical and chemical barriers to cell penetration (Aist 1976; Schmelzer 2002; Hardham et al. 2008). However, syncytia continue their later stages of the resistant reaction even at 7 dpi in *G. max*$_{[Peking]}$ (Riggs et al. 1973). The resistant reaction is accompanied by the degeneration of the p-J2 nematode within 4–5 dpi (Endo 1964, 1965; Kim et al. 1987; Kim and Riggs 1992). Consequently, the *G. max*$_{[Peking]}$-type of resistance response blocks *H. glycines* development at the p-J2 stage (Endo 1965; Riggs et al. 1973).

In contrast, studies in a derivative of *G. max*$_{[PI\ 88788]}$, known as *G. max*$_{[Bedford/PI\ 548974]}$ revealed a different cytological response (Hartwig and Epps 1978). The *G. max*$_{[Bedford/PI\ 548974]}$ resistance reaction lacks the development of a necrotic layer by 5 dpi (Kim et al. 1987). This is an important distinction between the *G. max*$_{[Peking]}$- and *G. max*$_{[PI\ 88788]}$ types of resistant reactions because a necrotic layer is formed in *G. max*$_{[Peking]}$. The initial stages of the *G. max*$_{[PI\ 88788]}$-type of resistant reaction involves extensive accumulation of cisternae and rough ER and nuclear degeneration within the syncytium by 5 dpi (Kim et al. 1987). There are no thickened cell walls or CWAs that form. Degradation of the cytoplasm is observed by 10 dpi (Kim et al. 1987). The *G. max*$_{[PI\ 88788]}$-type of resistance reaction results in nematode death at the J3 and J4 stages (Acido et al. 1984; Kim et al. 1987; Colgrove and Niblack 2008) which is later than that observed for the *G. max*$_{[Peking]}$-type of reaction.

The observations demonstrate that the *G. max*$_{[Peking]}$-type of resistance reaction is potent and rapid while the *G. max*$_{[PI\ 88788]}$-type is potent but prolonged. The research shows the merit of categorizing resistance as the *G. max*$_{[Peking]}$-type or the *G. max*$_{[PI\ 88788]}$-type. This is because it places the reactions into a useful context at the cellular and developmental levels for both the plant and the parasite. By knowing the chronology of the reactions, the time points can be used as benchmarks for the design of gene expression experiments that can test what underlies the different forms of the resistant reactions. To perform these studies, reliable methods are required to isolate the nurse cells undergoing the resistant reactions.

Important molecular information on the details of the resistant reactions of plants to parasitic nematodes has been obtained by isolating syncytia by laser capture microdissection (LCM) (Klink et al. 2005, 2007b, 2009c, 2010a, b). The LCM procedure is a proven method to faithfully isolate homogeneous cell populations from complex tissue (Isenberg et al. 1976; Meier-Ruge et al. 1976; Emmert-Buck et al. 1996; Asano et al. 2002). The LCM-based studies investigating the resistant reaction occurring at the site of infection were accompanied by molecular and computational investigations (Klink et al. 2005, 2007a, 2009a, 2010a, b). RNA isolated from syncytia undergoing resistant or susceptible reactions has been used to make cDNA libraries and clone full length genes (Klink et al. 2005). The cDNAs synthesized from microdissected syncytia has been used for making probes for RNA in situ hybridization and to perform quantitative measures of gene expression (qRT-PCR) (Klink et al. 2005). RNA isolated from syncytia has also been used to compare resistant and susceptible reactions in microarray analyses (Klink et al. 2007a, 2009a, 2010a, b). Some of these studies have relied on multiple genetically distinct *H. glycines* populations to obtain resistant or susceptible reactions in a single *G. max* genotype (Klink et al. 2007a, 2009a, 2010b). Such experiments provide an unambiguous comparative analysis of resistant and susceptible reactions because no genetic differences exist in the plant genotype. The analyses identified many induced and suppressed genes and gene pathways in *G. max*$_{[Peking/PI\ 548402]}$ and *G. max*$_{[PI\ 88788]}$ as compared to their respective genotype-specific pericycle and surrounding cell populations (Klink et al. 2007a, 2009a, 2010a). Prior analyses identified differential expression in the form of induced gene expression where expression is measurably higher in the syncytium than a control population of cells during a resistant reaction (Klink et al. 2007a, 2009a, 2010a). The analyses also identified differential expression in the form of suppressed gene activity where expression is measurably lower than a control population of cells during a resistant reaction (Klink et al. 2007a, 2009a, 2010a). The analyses have identified induced levels of genes involved in lipoxygenase signaling and phenylpropanoid metabolism among others (Klink et al. 2007a, 2009a, 2010a). While

these studies have revealed some of the intricacies of the individual resistant reactions occurring in the *G. max*$_{[Peking/PI\ 548402]}$ and *G. max*$_{[PI\ 88788]}$ genotypes, they did not provide a comparative analysis of the different forms of the resistant reaction.

Since comparative studies between the different forms of the resistant reaction have not been done, analyses of modulations in gene expression that relate to the different forms of the resistant reaction could not be addressed. Modulation is defined as changes in gene activity that are based on the genotype of the plant, in the case presented here, the form of the resistant reaction. Modulation is a property that is different than differential expression. Modulation is different because in modulation, the activity state of the gene pertains to a specific point of time during a developmental process in comparisons between different genotypes. Thus, a gene can experience differential expression (i.e., an induced state) as compared to a control cell population while also being amplified in its expression as compared to a different *G. max* genotype (i.e., *G. max*$_{[Peking/PI\ 548402]}$ vs. *G. max*$_{[PI\ 88788]}$). Alternatively, the modulated gene activity can be attenuated. Attenuation is defined as the activity of a gene being lower in one genotype as compared to the other. Thus, a gene can be experiencing induced activity and also be attenuated in comparisons between different genotypes at a specific time point.

Research on the genetic program underlying how a single genetically pure, inbred population of *H. glycines* elicits the development of two very different forms of the resistant reaction at the site of infection would determine commonalities and unique features of the different reactions. This is an important point because the genetic program accompanying the contrasting resistant reactions involves a dramatic change in the rate of the reaction that is dependent on the genotype of plant that is infected. Comparative analyses of the different forms of the resistant reaction can be done by using *G. max*$_{[Peking/PI\ 548402]}$ and *G. max*$_{[PI\ 88788]}$ because they have been extensively studied at the cytological level.

The microarray analysis presented here compares the resistance processes of *G. max*$_{[Peking/PI\ 548402]}$ and *G. max*$_{[PI\ 88788]}$. This work represents a unique perspective on how gene expression is occurring during the resistant reaction in two soybean genotypes that both share while also having unique sets of resistance genes. Importantly, a single *H. glycines* race, *H. glycines*$_{[NL1\text{-}RHg]}$, determined to be HG-type 7 (race 3) (Klink et al. 2007a, 2009a, 2010a) is used to obtain the diverse resistant reaction types observed in *G. max*$_{[Peking/PI\ 548402]}$ and *G. max*$_{[PI\ 88788]}$. The time points selected for the analysis span both the parasitism and resistance phases of the resistant reaction (Klink et al. 2009a, 2010a).

The work moves beyond prior investigations by showing genes and gene pathways that experience differential expression and modulated gene activity. This was accomplished because the analyses investigated the rapid and potent resistant reaction of *G. max*$_{[Peking/PI\ 548402]}$ as compared to the prolonged but potent resistant reaction of *G. max*$_{[PI\ 88788]}$. These observations answer the question of whether modulated gene expression underlies the *G. max*$_{[Peking/PI\ 548402]}$ and *G. max*$_{[PI\ 88788]}$ forms of the resistant reaction. The work also identifies differential gene expression that is common between the *G. max*$_{[Peking/PI\ 548402]}$ and *G. max*$_{[PI\ 88788]}$ genotypes. This work in its entirety shows that all localized resistant reactions at the syncytium of the different *G. max* genotypes are not under the same genetic control and/or involve the same genomic imprint. The work also shows that a common gene expression pattern is present between *G. max*$_{[Peking/PI\ 548402]}$ and *G. max*$_{[PI\ 88788]}$ that may represent a generalized physiological platform in action that underlies a broad spectrum resistance to *H. glycines*.

Materials and methods

Experimental methods

The materials and methods pertaining to *H. glycines* populations, *G. max* genotypes, experimental procedures and data analyses are published in Klink et al. 2009a and Klink et al. 2010a.

Plant and nematode procurement

Plant and nematode procurement methods are published (Klink et al. 2005, 2007a, b, 2009a, b, c, 2010a, b; Alkharouf et al. 2006). The plant introduction (PI) identifier for *G. max*$_{[Peking]}$ genotype used in the analyses is PI 548402 (*G. max*$_{[Peking/PI\ 548402]}$). The PI identifier for *G. max*$_{[Peking]}$ is important because it has seven different plant introductions (PI 297543, PI 438496 A, PI 438496 B, PI 438496 C, PI 438497, PI 548402S) of unclear association. Unlike *G. max*$_{[Peking]}$, *G. max*$_{[PI\ 88788]}$ is unique. The *G. max*$_{[Peking/PI\ 548402]}$ and *G. max*$_{[PI\ 88788]}$ stocks were originally obtained from a seed bank that is managed and maintained by the United States Department of Agriculture (USDA). Seeds were made available through the National Plant Germplasm System (http://www.ars-grin.gov/npgs/acc/acc_queries.html). The *H. glycines* NL1-RHg population used in the studies is race 3, HG-type 7 (*H. glycines*$_{[NL1\text{-}RHg/HG\text{-}type\ 7]}$) as determined in the independent lab of Dr. Terry Niblack (Department of Crop Sciences, University of Illinois) June–July 2007 using the methods of Niblack et al. (2002) (Klink et al. 2009a, 2010a).

The HG-type test also determined that *G. max*$_{[Peking/PI\ 548402]}$ and *G. max*$_{[PI\ 88788]}$ are considered highly resistant to *H. glycines*$_{[NL1\text{-}RHg/HG\text{-}type\ 7]}$ (Klink et al. 2009a, 2010a). Consistency of the performance of *G. max*$_{[Peking/PI\ 548402]}$ and *G. max*$_{[PI\ 88788]}$ genotypes are tested and confirmed for each experiment (Klink et al. 2009a, 2010a). The *G. max*$_{[Peking/PI\ 548402]}$ and *G. max*$_{[PI\ 88788]}$ genotypes are used in the experiments to obtain resistant reactions by the use of *H. glycines*$_{[NL1\text{-}RHg/HG\text{-}type\ 7]}$. The *H. glycines*$_{[NL1\text{-}RHg/HG\text{-}type\ 7]}$ population is maintained in the greenhouse using the moisture replacement system (Sardanelli and Kenworthy 1997). Prior to infection, the nematodes are diluted to a final concentration of 2,000 pi-J2/ml. This quantity of nematodes is added to each root of each plant. The roots, including the mock-infected control samples, are washed after 1 day to remove nematodes that had not penetrated the roots. Infected roots are grown for 3, 6 or 9 dpi. Maximally infected lateral roots are harvested for analyses. The process is subsequently repeated twice, providing three independent sets of samples.

Histology

Histological observation is performed according to Klink et al. (2005, 2007a, b, 2009a, b, c, 2010a, b). Briefly, tissue is fixed in Farmer's solution (FS) composed of 75% ethanol, 25% acetic acid (Sass 1958; Klink et al. 2005). Tissue is cast and subsequently mounted for sectioning. Serial sections of roots are made on an American Optical 820® microtome (American Optical Co®.; Buffalo, NY, USA) at a section thickness of 10 µm. Sections are stained in a manner similar to the original experiments of Ross (1958) and Endo (1965). Staining involves Safranin O (Fisher Scientific Co.; Fair Lawn, NJ, USA) in 50% ETOH and counter-staining in Fast Green FCF (Fisher Scientific Co.) (Klink et al. 2005). For histological analyses, the tissue is permanently mounted in Permount® (Fisher Scientific Co.).

LCM and microarray hybridization

Slides are prepared according to Klink et al. (2005, 2007a, 2009a, 2010a, b). LCM is performed on a Leica® ASLMD microscope® (Leica®). Syncytia are simple to visualize (Fig. 2) and microdissect (Fig. 3). What is difficult to do is estimate the actual number of cells used in the studies. This is because serial sections of paraffin-embedded tissue were used for LCM of the control and syncytium cells. In addition, by definition, the syncytium is composed of multiple fused cells that are difficult to differentiate from each other. Also, the cells under study were undergoing a resistant reaction, complicating visualization of the individual cells that compose the syncytium. Serial sections of approximately 100 syncytia were used to obtain the RNA for the studies for each replicate. Seven sub-replicates were made for each replicate. Over 100 ng of RNA per replicate was obtained for the studies. Work to obtain RNA is done with the PicoPure RNA Isolation kit (Molecular Devices® [formerly Arcturus®]; Sunnyvale, CA, USA, Cat. # KIT0204). A DNAse treatment is added, just before the second column wash, using DNAfree® (Ambion®, Austin, TX, USA). RNA quality and yield are determined using the RNA 6000 Pico Assay® (Agilent Technologies®, Palo Alto, CA, USA) using the Agilent 2100 Bioanalyzer® according to the manufacturer's instructions. Both probe preparation and hybridization procedures on the GeneChip® Soybean Genome Array (Affymetrix®, Cat. # 900526) was performed according to Affymetrix® guidelines.

Data analysis

The soybean GeneChip® data is imported and analyzed using the MATLAB Bioinformatics Toolbox (Mathworks Inc.; Natick, MA, USA). Log2 scaling is used to standardize the dataset. Volcano plots are produced using samples having a fold change of $\geq|\pm 1.5|$ and also having a P value ≤ 0.05 as compared to the control (Alkharouf et al. 2006) and false discovery rate (FDR) less than 10% (Klink et al. 2009a, 2010a). Annotations are made by comparison to the *Arabidopsis thaliana* gene ontology (GO) database (The Gene Ontology Consortium 2004) based on their best match obtained by BLAST searches (Altschul et al. 1997). Annotations were subsequently re-run in order to identify additional best-hit matches. Annotations were updated September 2010.

Gene pathway analyses

The pathway analysis visualizes pathways according to Kyoto Encyclopedia of Genes and Genomes (KEGG) (http://www.genome.jp/kegg/catalog/org_list.html) from Affymetrix® gene expression data. In the pathway analysis, the darker the shade of green represents the greater the level of induced gene expression as compared to controls or amplified expression as compared to the other genotype. Yellow represents expressed. The darker the shade of red means the greater the suppressed level gene expression or lower expression as compared to the other genotype. Data supplemental to each table and figure and GO terms (The Gene Ontology Consortium 2004) are available (http://bioinformatics.towson.edu//).

Results

Histology

The resistant reaction at the syncytium undergoes two phases during its development that leads to mortality of the

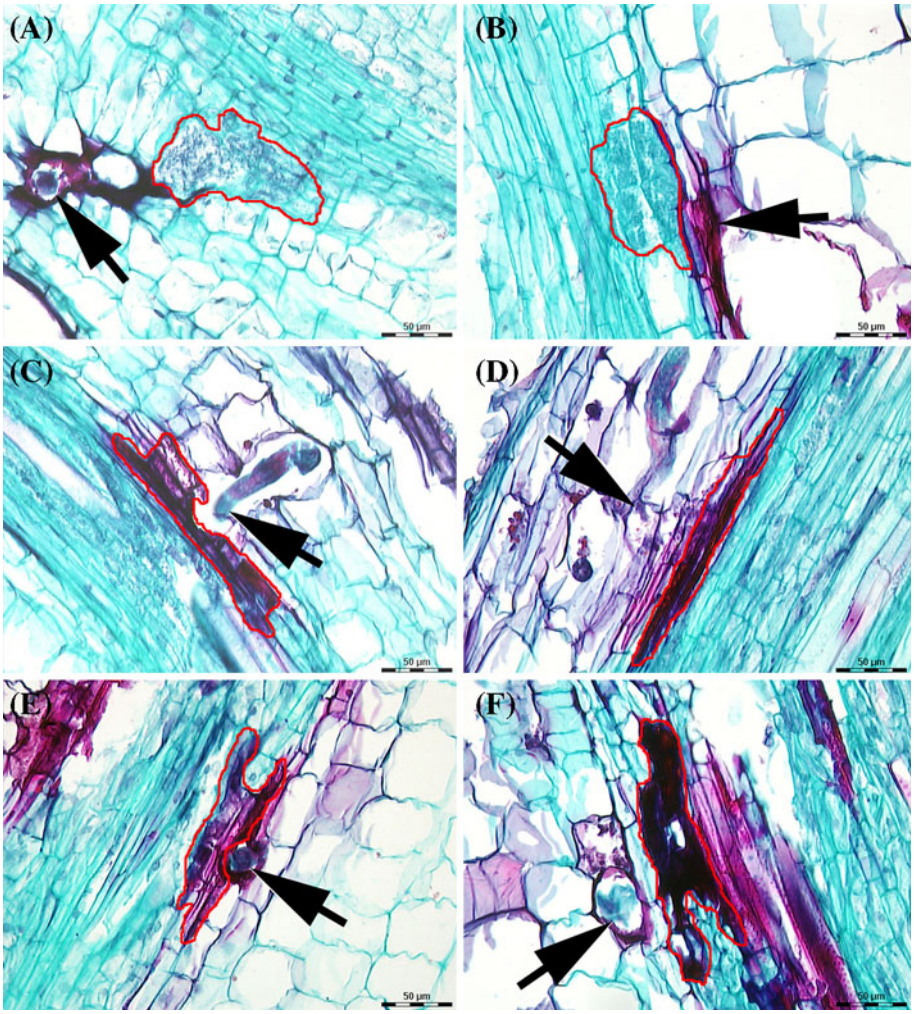

Fig. 2 Histological responses of *G. max*$_{[Peking/PI\ 548402]}$ and *G. max*$_{[PI\ 88788]}$ roots to *H. glycines* infection during their resistant reactions. **a** *G. max*$_{[Peking/PI\ 548402]}$ at 3 dpi. **b** *G. max*$_{[PI\ 88788]}$ at 3 dpi. **c** *G. max*$_{[Peking/PI\ 548402]}$ at 6 dpi. **d** *G. max*$_{[PI\ 88788]}$ at 6 dpi. **e** *G. max*$_{[Peking/PI\ 548402]}$ at 9 dpi. **f** *G. max*$_{[PI\ 88788]}$ at 9 dpi. *Arrow*, nematode, *red line*, perimeter of syncytium

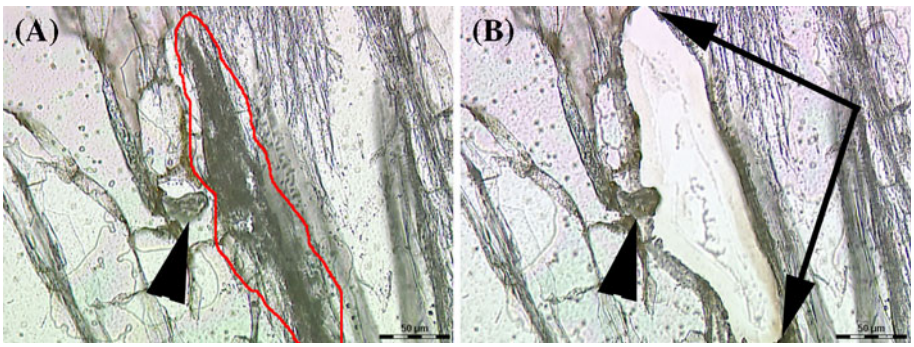

Fig. 3 A microdissected syncytium. **a** Before LCM; **b** after LCM. Red line, perimeter of the syncytium. *Black arrow*, head of nematode, *white arrows*, microdissected syncytium

nematode (Fig. 1). The first phase (phase 1) is a parasitism phase whereby the nematode infects a cell and establishes the initial stages of syncytium development. The second phase (phase 2) is the resistance phase whereby syncytia collapse and cease to function. The parasitism phase is prolonged during a susceptible reaction, presumably by overriding the resistance phase. That activity results in a compatible interaction with the *G. max* genotype. Histological examination of syncytia is aided by the safranin-Fast Green staining procedure (Sass 1958; Ross 1958; Endo 1965; Klink et al. 2005, 2007a, b, 2009a, 2010a, b). Safranin is a regressive stain, known to preferentially stain lignified, suberinized and cutinized tissues as well as staining chromosomes and nucleoli red. In contrast, the progressive counterstain Fast Green is known to preferentially stain cytoplasm and cellulosic cell walls. Histological examination of roots used in the analyses demonstrates that *G. max*$_{[Peking/PI\ 548402]}$ and *G. max*$_{[PI\ 88788]}$ roots are

infected with *H. glycines*[NL1-RHg/HG-type 7] at 3 dpi (Fig. 2a, b), 6 dpi (Fig. 2c, d) and 9 dpi (Fig. 2e, f), respectively. The walls of cells undergoing the parasitism stage appear to stain for cellulose in both *G. max*[Peking/PI 548402] (Fig. 2a) and *G. max*[PI 88788] (Fig. 2b). In contrast, the walls of the resistance phase of the resistant reaction appear to stain preferentially for lignin, suberin and/or cutin in *G. max*[Peking/PI 548402] (Fig. 2c, e) and *G. max*[PI 88788] and (Fig. 2e, f). This staining characteristic is also observed by Ross (1958), Endo (1965) and Klink et al. (2007a, b, 2009a, 2010a, b). Identification of syncytia is a simple diagnostic that was applied to the LCM analyses (Fig. 3a, b).

Direct comparison of *G. max*[Peking/PI 548402] to *G. max*[PI 88788] syncytium gene expression

Prior analyses have identified genes that are induced or suppressed in the syncytia of *G. max*[Peking/PI 548402] (Klink et al. 2007a, 2009a) and *G. max*[PI 88788] (Klink et al. 2010a) undergoing their respective resistant reactions. However, it is known that the *H. glycines*[NL1-RHg/HG-type 7] population elicits two distinctly different resistant reactions in the *G. max*[Peking/PI 548402] and *G. max*[PI 88788] genotypes as it attempts to develop a functional syncytium. Thus, from the prior analyses, a gap in knowledge is the direct cross comparison of the *G. max*[Peking/PI 548402] and *G. max*[PI 88788] resistant reactions. The aim of the direct comparative analyses is examining relative levels of gene activity present in syncytia of the potent and rapid resistant reaction of *G. max*[Peking/PI 548402] as compared to the potent but prolonged resistant reaction of *G. max*[PI 88788] genotype (base line). Since *G. max*[PI 88788] is used as the base line, the output for all of the experiments presented in the analysis is relative expression for *G. max*[Peking/PI 548402].

The first set of experiments compare relative levels of gene expression in pericycle and surrounding cells prior to infection (Fig. 4a) and from microdissected syncytia at the 3 (Fig. 4b), 6 (Fig. 4c) and 9 dpi (Fig. 4d). As expected, the experiments reveal that much of the measurable relative levels of gene expression occurring between the *G. max*[Peking/PI 548402] and *G. max*[PI 88788] genotypes is similar. Therefore, the experiments show the robustness of the relative expression data for thousands of genes in two different genotypes. However, a smaller amount of gene expression is found to be significantly different between the *G. max*[Peking/PI 548402] and *G. max*[PI 88788] genotypes. The observation reveals that amplitude differences in expression exist between the potent and rapid *G. max*[Peking/PI 548402] resistant reaction and the potent but prolonged resistant reaction of *G. max*[PI 88788].

G. max[Peking/PI 548402] pericycle cells have amplified levels of genes pertaining to defense pathways prior to infection

The direct comparative analyses of the pericycle and surrounding cells isolated from uninfected roots identified a probe set for the differentially expressed in response to arachidonic acid 1 gene (*DEA1* [*Gm*-DEA1]) (CA850542) to measure the greatest difference in relative gene expression (224.19-fold) when comparing *G. max*[Peking/PI 548402] to *G. max*[PI 88788]. A second probe set measuring higher relative levels of gene expression was a protease inhibitor (BU082252) (68.28-fold). Other probe sets with high relative expression levels greater than 20-fold in *G. max*[Peking/PI 548402] include 3 polygalacturonidases (CF808466, CD414773, AF128266), an R-gene (BI785070), 2 lipoxygenases (CD409280, BM092012), EMBRYO DEFECTIVE 1374 (CD401715), Zwille-like protein (BG651396) and ACC oxidase (BE440266) (Table 1; Supplemental Table 1). Probe sets measuring relatively lower levels of gene expression in *G. max*[Peking/PI 548402] were also identified (Supplemental Table 1).

G. max[Peking/PI 548402] syncytia have amplified levels of genes pertaining to defense pathways during the resistant reaction

Expression analyses followed that compare *G. max*[Peking/PI 548402] syncytium gene expression directly to *G. max*[PI 88788] syncytium gene expression at the 3 dpi (Fig. 4b; Supplemental Table 2), 6 dpi (Fig. 4c; Supplemental Table 3) and 9 dpi time points (Fig. 4d; Supplemental Table 4). The analyses identify differences in gene expression both prior to and during both phase 1 and phase 2 of the resistant reactions. Pathway analyses are presented in the next section.

Pathway analyses identify amplified levels of genes in *G. max*[Peking/PI 548402] syncytia as compared directly to *G. max*[PI 88788] at 3 dpi

Differences in gene expression amplitude were observed between the *G. max*[Peking/PI 548402] and *G. max*[PI 88788] genotypes (Fig. 4), However, what was not easy to determine from the gene annotation analyses of individual genes presented in Fig. 4 was whether specific gene pathways were amplified in their activity in one genotype as compared to the other. The context in which those genes function would likely become more obvious through pathway analyses.

Pathway analyses were made from the direct comparative analyses of *G. max*[Peking/PI 548402] and *G. max*[PI 88788] syncytia undergoing the resistant reaction at 3 dpi as

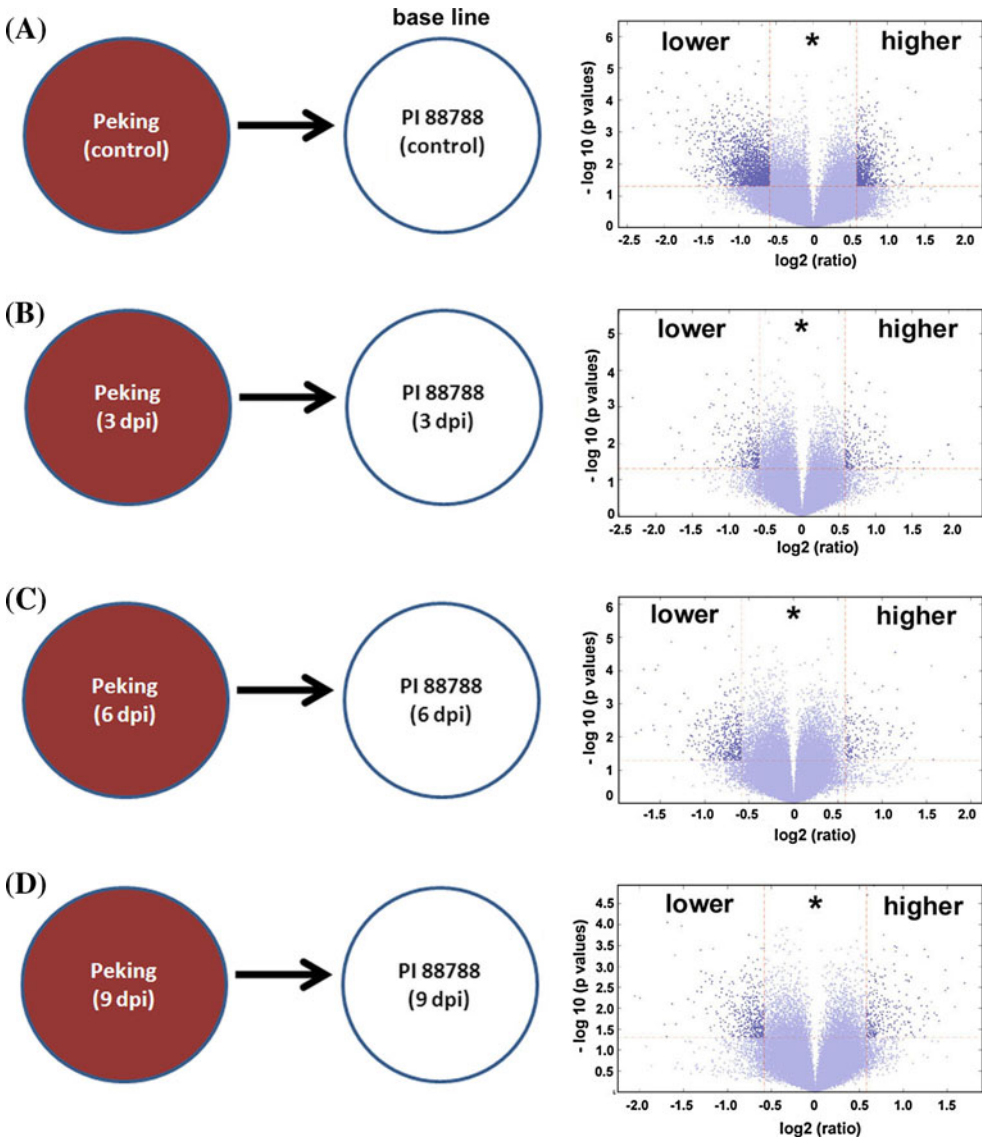

Fig. 4 Volcano plots depicting relative gene expression. To the left of the volcano plot is a graphic depicting the comparison being made. The gene expression of *G. max*$_{[PI\ 88788]}$ is the base line of the comparisons. Therefore, expression is presented in terms of relative levels in *G. max*$_{[Peking/PI\ 548402]}$. **a** The *G. max*$_{[Peking/PI\ 548402]}$ pericycle isolated from uninoculated roots vs. *G. max*$_{[PI\ 88788]}$ pericycle (baseline) that was isolated from uninoculated roots. **b** 3 dpi *G. max*$_{[Peking/PI\ 548402]}$ syncytium vs. 3 dpi *G. max*$_{[PI\ 88788]}$ syncytium. **c** 6 dpi *G. max*$_{[Peking/PI\ 548402]}$ syncytium vs. 6 dpi *G. max*$_{[PI\ 88788]}$ syncytium. **d** 9 dpi *G. max*$_{[Peking/PI\ 548402]}$ syncytium vs. 9 dpi *G. max*$_{[PI\ 88788]}$ syncytium. A $\geq|\pm 1.5|$ fold cutoff and $P \leq 0.05$ with a FDR set at 12% was used for the analyses. Genes with higher relative levels of expression (*dark blue*, *upper right quadrant*) and genes with lower relative levels of expression (*dark blue*, *upper left quadrant*) in *G. max*$_{[Peking/PI\ 548402]}$ are presented. Genes with no statistically significant differences in expression used later in the combined analyses are denoted by an *asterisk* (*)

compared to their respective pericycle and surrounding cells (base line). The analyses identified induced levels of components of the brassinosteroid signaling pathway in both *G. max*$_{[Peking/PI\ 548402]}$ (Fig. 5a; Supplemental Fig. 1A) and *G. max*$_{[PI\ 88788]}$ (Fig. 5b; Supplemental Fig. 1B), some components of the fatty acid biosynthesis pathway (Supplemental Fig. 1C, D), glycolysis (Supplemental Fig. 1E, F), components of the phenylpropanoid biosynthesis pathway (Supplemental Fig. 1G, H) and ubiquinone and terpenoid-quinone biosynthesis pathways (Supplemental Fig. 1I, J). With this information in hand, it was then possible to see whether amplified levels of these induced genes/pathways existed in *G. max*$_{[Peking/PI\ 548402]}$ as compared directly to *G. max*$_{[PI\ 88788]}$ at 3, 6 and 9 dpi (see below).

At 3 dpi, pathway analyses revealed induced and amplified levels of genes in the brassinosteroid signaling pathway in *G. max*$_{[Peking/PI\ 548402]}$ as compared directly to *G. max*$_{[PI\ 88788]}$ (Fig. 5c; Supplemental Fig. 2A), anthocyanin biosynthetic pathway (Supplemental Fig. 2B), benzoxazinoid pathway (Supplemental Fig. 2C), fatty acid biosynthesis (Supplemental Fig. 2D), glycosphingolipid metabolism (Supplemental Fig. 2E), high mannose type *N*-glycan biosynthesis (Supplemental Fig. 2F), components of the phenylpropanoid biosynthesis pathway (Supplemental Fig. 2G), stilbenoid, diarylhepatanoid and gingerol biosynthesis (Supplemental Fig. 2H) and ubiquinone and terpenoid-quinone biosynthesis pathways (Supplemental Fig. 2I). The results show that while many of these genes are induced in each genotype as compared to their respective pericycle and surrounding cell controls, amplitude differences do exist in *G. max*$_{[Peking/PI\ 548402]}$ as compared to *G. max*$_{[PI\ 88788]}$ for components of pathways involved in important aspects of metabolism and defense. All 3 dpi direct comparison pathways can be found at the

Table 1 A comparative analysis of *G. max*$_{[Peking/PI\ 548402]}$ pericycle to *G. max*$_{[PI\ 88788]}$ (baseline) pericycle, identifying genes with higher relative levels of expression

Probe ID	GenBank ID	Description	FC	PV	*q* value (%)
Peking pericycle-induced					
GmaAffx.80464.1.S1_at	CA850542	Arachidonic acid-induced DEA1	224.1921	4.14E-05	0
Gma.677.1.S1_at	BU082252	Protease inhibitor	68.27514	7.46E-04	0
GmaAffx.92741.1.S1_s_at	CF808466	Polygalacturonase-like protein	66.07655	7.17E-03	0
Gma.1043.1.S1_at	BI785070	R-gene	55.06712	5.68E-05	0
Gma.17364.1.S1_at	CA803078	P24 oleosin isoform A	53.78355	2.46E-04	0
Gma.7993.1.S1_at	BI967267	Extensin-like protein	49.69328	1.38E-05	0
Gma.5315.1.S1_at	CD409280	Lipoxygenase, LH2	44.88481	2.14E-04	0
GmaAffx.16632.1.S1_at	AW598371	NA	39.42695	8.56E-03	0.4497689
GmaAffx.71067.1.S1_at	AW307334	NA	38.62491	1.66E-02	0.2361532
Gma.3308.1.S1_at	CD414773	Polygalacturonase-like protein	37.9182	5.46E-05	0
GmaAffx.11899.1.A1_at	AW759403	Glycosyl hydrolase family 1 protein	35.06023	7.18E-05	0
Gma.16558.1.S1_at	CD401715	ATSUFE/CPSUFE/EMB1374 (EMBRYO DEFECTIVE 1374)	31.79591	8.06E-03	0
GmaAffx.88165.1.S1_at	BE583573	STP1 (SUGAR TRANSPORTER 1)	31.15182	1.19E-02	0
GmaAffx.27712.1.S1_at	AW707016	NA	29.18668	1.39E-05	0
GmaAffx.73486.1.S1_s_at	BM092012	Lipoxygenase, LH2	28.98119	5.81E-03	0
Gma.15398.1.S1_at	BG651396	Zwille protein-like	27.62509	1.52E-03	0
Gma.8494.1.S1_at	AF128266	Polygalacturonase PG1	27.43525	1.05E-02	0.3437161
Gma.6146.1.S1_at	BI969869	Putative 14-kDa proline-rich protein	27.41625	2.21E-03	0
Gma.3591.1.S1_a_at	BE440266	ACC oxidase	25.51494	2.80E-02	0.8628225
GmaAffx.75044.1.A1_at	CD397448	NA	24.84929	5.02E-04	0
GmaAffx.69913.1.A1_at	BU550803	NA	24.21203	1.86E-03	0
Gma.2505.1.S1_at	AB062754	Ferritin-2, chloroplast precursor	21.16031	1.50E-02	0
Gma.684.2.A1_at	BU084534	Cold acclimation WCOR413	21.04413	2.67E-02	0.3437161
Gma.8299.1.S1_at	BI967830	Protein phosphatase-2c	20.57819	4.42E-03	0.2361532
Gma.772.1.S1_at	BE819852	Hypothetical protein	20.57294	2.66E-04	0
GmaAffx.36115.1.A1_at	BE659438	NA	20.4504	1.05E-03	0
GmaAffx.80486.1.S1_at	AW733824	Pectin acetylesterase	20.17877	8.96E-03	0.2361532
GmaAffx.49549.1.S1_at	BG363167	Synaptobrevin-related	20.16506	1.14E-03	0
GmaAffx.65885.1.A1_at	CD405808	Zinc finger (C2H2 type)	20.12014	4.78E-03	0.2361532
GmaAffx.9605.1.S1_at	BM091603	NA	20.09384	6.03E-04	0

FC Fold change, *PV P* value. A $\geq|\pm 1.5|$ fold cutoff and $P \leq 0.05$ was used. FDR was set to 12%. The probe set satisfied the criteria set by the differential expression and FDR analyses. Full gene lists are Supplemental Table 1

Supplemental Data Link: 3 dpi pathway analysis. Similar direct comparative analyses of the *G. max*$_{[Peking/PI\ 548402]}$ and *G. max*$_{[PI\ 88788]}$ genotypes were expanded to the 6 and 9 dpi time points.

Pathway analyses identify amplified levels of genes in *G. max*$_{[Peking/PI\ 548402]}$ syncytia as compared directly to *G. max*$_{[PI\ 88788]}$ at 6 dpi

Pathway analyses were done that directly compared 6 dpi *G. max*$_{[Peking/PI\ 548402]}$ syncytia to 6 dpi *G. max*$_{[PI\ 88788]}$ syncytia. At 6 dpi, amplified levels of genes in the anthocyanin biosynthesis pathway (Supplemental Fig. 3A), glycosphingolipid (Supplemental Fig. 3B) and high mannose type *N*-glycan biosynthesis (Supplemental Fig. 3C) were observed. In contrast, suppressed levels of brassinosteroid biosynthesis (Supplemental Fig. 3D), fatty acid biosynthesis (Supplemental Fig. 3E) and phenylpropanoid pathways (Supplemental Fig. 3F) were observed. All 6 dpi direct comparison pathways can be found at the Supplemental Data Link: 6 dpi pathway analysis.

Pathway analyses identify amplified levels of genes in *G. max*$_{[Peking/PI\ 548402]}$ syncytia as compared directly to *G. max*$_{[PI\ 88788]}$ at 9 dpi

Pathway analyses were done that directly compared 9 dpi *G. max*$_{[Peking/PI\ 548402]}$ syncytia to 9 dpi *G. max*$_{[PI\ 88788]}$

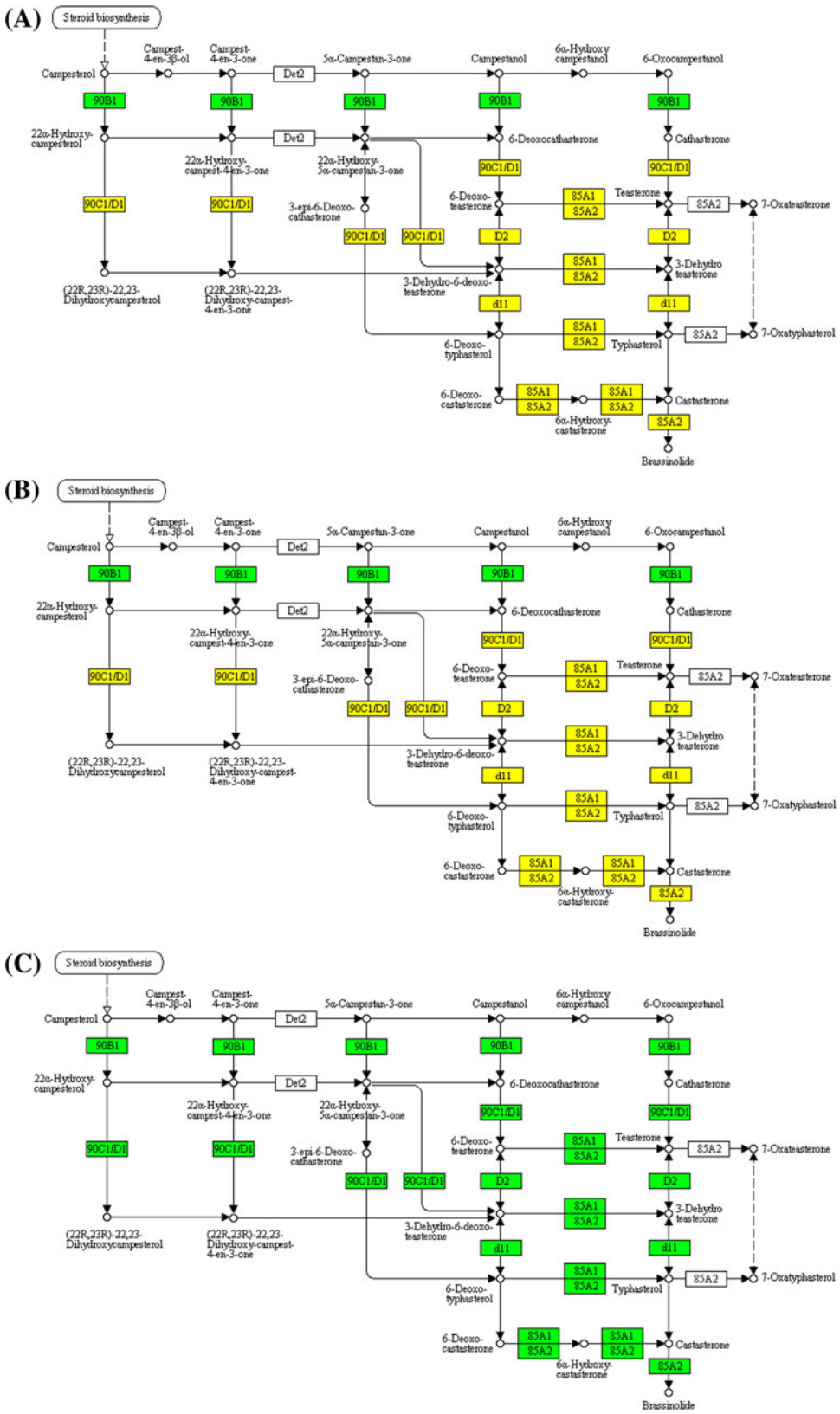

Fig. 5 Pathway analysis and comparison of the brassinosteroid biosynthesis pathway. **a** The brassinosteroid biosynthesis pathway in *G. max*$_{[Peking/PI\ 548402]}$ 3 dpi syncytia gene expression as compared to *G. max*$_{[Peking/PI\ 548402]}$ pericycle and surrounding cells. **b** The brassinosteroid biosynthesis pathway in *G. max*$_{[PI\ 88788]}$ 3 dpi syncytia gene expression as compared to *G. max*$_{[PI\ 88788]}$ pericycle and surrounding cells. **c** The brassinosteroid biosynthesis pathway in *G. max*$_{[Peking/PI\ 548402]}$ 3 dpi syncytia gene expression as compared to the brassinosteroid biosynthesis pathway in *G. max*$_{[PI\ 88788]}$ 3 dpi syncytia

syncytia. At 9 dpi, amplified levels of genes in the anthocyanin biosynthetic pathway (Supplemental Fig. 4A), alpha linoleic acid metabolism pathway (Supplemental Fig. 4B), fatty acid elongation in mitochondria pathway (Supplemental Fig. 4C), glycosphingolipid biosynthesis pathway (Supplemental Fig. 4D), Fatty acid metabolism pathway (Supplemental Fig. 4E), high mannose type *N*-glycan biosynthesis pathway (Supplemental Fig. 4F), peptidoglycan biosynthesis pathway (Supplemental Fig. 4G), metabolism of xenobiotics by cytochrome P450 (Supplemental Fig. 4H), ubiquinone and terpenoid-quinone biosynthesis pathways (Supplemental Fig. 4I). Relatively lower levels of the brassinosteroid biosynthesis pathway (Supplemental Fig. 4J) and carotenoid biosynthetic pathways (Supplemental Fig. 4K) were observed. While components of important defense pathways are induced in either *G. max*$_{[Peking/PI\ 548402]}$ or *G. max*$_{[PI\ 88788]}$ as compared to their respective pericycle and surrounding cells, the observations demonstrate further that amplitude differences exist between the *G. max*$_{[Peking/PI\ 548402]}$ genotype as compared to *G. max*$_{[PI\ 88788]}$. All 9 dpi direct comparison pathways can be found at the Supplemental Data Link: 9 dpi pathway analysis.

Differences in relative levels of gene expression are sustained throughout the resistant reaction of *G. max*$_{[Peking/PI\ 548402]}$ or *G. max*$_{[PI\ 88788]}$ during the 3, 6 and 9 dpi time points

The aforementioned analyses were time point specific and did not address whether the amplitude differences in gene expression spanned the duration of the resistant reactions of *G. max*$_{[Peking/PI\ 548402]}$ or *G. max*$_{[PI\ 88788]}$. Analyses were done to compare the relative gene expression levels occurring between *G. max*$_{[Peking/PI\ 548402]}$ and *G. max*$_{[PI\ 88788]}$ at the 3, 6 and 9 dpi time points. This period represents the time course of infection. In these highly stringent analyses, to have sustained modulated gene expression, the criteria for amplified (consistently higher) or attenuated (consistently lower) levels of expression are satisfied when the probe set measures expression in a similar manner in the 9 biological replicates across the two genotypes (i.e., 3 biological replicates $\times$ 3 time points $\times$ 2 genotypes; FC $\geq$ 1.5, $P \leq 0.05$ and FDR $\leq$ 10%) for a total of 18 arrays. As expected, most probe sets did not measure differences in the level of expression between the two genotypes at all time points due to the stringency of the analysis. However, the analyses resulted in the identification of 93 probe sets measuring consistently and statistically significant differences in relative levels of gene expression in *G. max*$_{[Peking/PI\ 548402]}$ as compared to the *G. max*$_{[PI\ 88788]}$ genotype at all time points. Of those 93 probe sets, 57 have higher relative levels of gene expression in *G. max*$_{[Peking/PI\ 548402]}$ at the 3, 6 and 9 dpi time points (Table 2; Supplemental Table 5). The analysis also identified 27 probe sets that measure lower relative levels of gene expression at the 3, 6 and 9 dpi time points in *G. max*$_{[Peking/PI\ 548402]}$ as compared to *G. max*$_{[PI\ 88788]}$ (Table 2; Supplemental Table 5). The analyses demon strate that while much of the relative levels of gene expression are similar between the *G. max*$_{[Peking/PI\ 548402]}$ and *G. max*$_{[PI\ 88788]}$ genotypes during infection, a smaller number of probe sets measure relative gene expression levels that are consistently and statistically higher or lower in *G. max*$_{[Peking/PI\ 548402]}$ as compared directly to the *G. max*$_{[PI\ 88788]}$ genotype, but only after infection of the root cells by *H. glycines*.

The identification of constitutive differences in relative levels of gene expression that are present between the *G. max*$_{[Peking/PI\ 548402]}$ and *G. max*$_{[PI\ 88788]}$ genotypes

The prior analyses identified genes that initially had similar levels of gene expression in the control cell populations of both *G. max*$_{[Peking/PI\ 548402]}$ and *G. max*$_{[PI\ 88788]}$ genotypes. These similar levels were followed by modulations in gene activity that could be measured between *G. max*$_{[Peking/PI\ 548402]}$ and *G. max*$_{[PI\ 88788]}$ genotypes only at 3, 6, 9 dpi. The analyses presented here included the pericycle and surrounding cell (control) time point samples with the 3, 6 and 9 dpi time points. The analyses identify a different pool of probe sets that measure differences in relative gene expression on 24 arrays (i.e., 3 biological replicates $\times$ time points $\times$ 2 genotypes; FC $\geq$ 1.5, $P \leq 0.05$ and FDR $\leq$ 10%), representing all the time points. The analysis was done to identify the list of genes that had different levels of expression that were attributed to the *G. max*$_{[Peking/PI\ 548402]}$ and *G. max*$_{[PI\ 88788]}$ genotypes. Since gene expression was always different both prior to and after infection, the relative level of expression likely was intrinsic to the genotype and not due to infection by *H. glycines*. The analyses identified 25 probe sets that measure consistently and statistically significant higher relative levels of gene expression in *G. max*$_{[Peking/PI\ 548402]}$ as compared to *G. max*$_{[PI\ 88788]}$ across the 4 time points (Table 3; Supplemental Table 6). The analysis also identified 5 additional probe sets that measured statistically significant lower relative levels of gene expression in *G. max*$_{[Peking/PI\ 548402]}$ as compared to *G. max*$_{[PI\ 88788]}$ at the 4 time points (Table 3; Supplemental Table 6).

Commonalities of the *G. max*$_{[Peking/PI\ 548402]}$ and *G. max*$_{[PI\ 88788]}$ resistant reactions

The previous analyses identified probe sets measuring different relative levels of gene expression occurring between

Table 2 A comparative time course analysis of *G. max*$_{[Peking/PI\ 548402]}$ 3, 6 and 9 dpi to *G. max*$_{[PI\ 88788]}$ (baseline) 3, 6 and 9 dpi resistant reaction

Probe ID	GenBank ID	Description	Control FC	3 day FC	6 day FC	9 day FC
HIGHER in G. max[Peking]						
GmaAffx.91687.1.A1_s_at	CF807412	Protein disulfide isomerase (PDI)-like protein 2	NA	16.42058	22.66097	16.55722
Gma.6245.1.S1_at	CA938361	Thaumatin	NA	15.98745	21.85067	11.51146
Gma.2044.1.S1_at	M94012	RESPONSIVE TO ABA 18 (RAB18)	NA	12.63209	19.24757	24.24861
GmaAffx.80465.1.S1_at	BU548370	ARABIDOPSIS THALIANA GALACTINOL SYNTHASE 2 (ATGOLS2)	NA	11.84203	7.204501	11.41504
Gma.11135.1.S1_at	AI856724	ATP-citrate lyase A-3 (ACLA-3)	NA	11.60219	3.023322	6.155099
Gma.3988.1.S1_at	BE658819	Lactoylglutathione lyase family protein	NA	9.953863	10.4648	9.34481
Gma.3473.1.S1_at	BQ628660	17.6 kDa class I small heat shock protein (HSP17.6B-CI)	NA	9.283021	4.034156	2.918122
Gma.391.1.A1_at	AW349964	Receptor-like protein kinase-related	NA	8.295254	3.48455	7.635437
GmaAffx.60625.1.S1_at	BQ740664	NA	NA	7.422014	4.368441	4.198288
Gma.2912.1.S1_at	AF117884	Late embryogenesis abundant protein (LEA)	NA	7.174836	6.243753	5.686975
Gma.173.1.S1_at	X63565	Late embryogenesis abundant group 1 (LEA1)	NA	6.270906	18.14174	6.578355
Gma.1950.1.S1_at	AF202184	Isoflavone reductase	NA	5.996244	2.927154	8.598727
Gma.2912.1.S1_s_at	AF117884	Late embryogenesis abundant protein (LEA)	NA	5.989421	12.04405	10.04885
Gma.4616.1.A1_at	AW349487	Thaumatin	NA	5.880116	5.885979	6.056813
GmaAffx.91687.1.S1_at	CF807412	Protein disulfide isomerase (PDI)-like protein 2	NA	5.820802	5.591163	4.333533
GmaAffx.15955.1.S1_at	AI495284	CPC (CAPRICE) transcription factor	NA	5.625248	5.174757	5.123017
Gma.12393.1.S1_a_at	BM093715	NINE-CIS-EPOXYCAROTENOID DIOXYGENASE3 (NCED3)	NA	5.587755	4.731004	3.145295
Gma.5637.1.S1_at	AY126715	ARABIDOPSIS THALIANA GALACTINOL SYNTHASE 1 (ATGOLS1)	NA	5.496911	7.509643	5.386323
LOWER in G. max[Peking]						
Gma.5949.1.A1_at	CD412339	Histone H3	NA	−48.089	−9.2502	−6.0738
GmaAffx.82904.1.S1_at	BM885134	NA	NA	−22.245	−9.11273	−8.6476
Gma.10969.3.S1_x_at	CD396552	Lipoxygenase	NA	−16.288	−16.2558	−4.7436
Gma.11166.1.S1_x_at	AW705829	Lipoxygenase 1 (LOX1)	NA	−12.04	−13.7154	−7.1331
Gma.6037.1.S1_at	CD390794	Hydroxycinnamoyl transferase	NA	−10.677	−26.6953	−15.725
Gma.7890.1.A1_at	AW309342	Pectinesterase family protein	NA	−8.6387	−6.53887	−4.8652
Gma.13208.2.A1_at	CD392188	ZPR 2 LITTLE ZIPPER 2	NA	−8.4889	−8.11234	−6.366
GmaAffx.54898.1.S1_s_at	BQ452830	Extensin	NA	−5.3104	−3.03486	−4.4452
Gma.3905.1.S1_at	BU547451	NA	NA	−4.6281	−2.51223	−6.4595
Gma.8520.1.S1_at	CA802722	Acid phosphatase, putative	NA	−4.628	−10.516	−12.966
GmaAffx.4050.1.S1_at	CD393498	Microtubule motor	NA	−3.7378	−5.2331	−4.4288
GmaAffx.73185.1.S1_at	BI701903	NA	NA	−3.0654	−7.76978	−6.1235
Gma.15577.1.S1_at	CD399075	NA	NA	−2.3505	−3.42822	−5.0828
GmaAffx.24622.1.S1_at	BU926989	NA	NA	−2.2107	−2.38433	−5.154

FC Fold change, *PV P* value. The analysis shows genes with higher relative levels of expression. A $\geq|\pm 1.5|$ fold cutoff and $P \leq 0.05$ was used. FDR was set to 12%. The probe set satisfied the criteria set by the differential expression and FDR analyses. Full information for the 3-point time course analysis (Supplemental Table 5) is provided

G. max$_{[Peking/PI\ 548402]}$ and *G. max*$_{[PI\ 88788]}$. However, the volcano plots demonstrate that a substantial number of probe sets are measuring similar relative levels of gene expression when directly comparing *G. max*$_{[Peking/PI\ 548402]}$ and *G. max*$_{[PI\ 88788]}$ (Fig. 4). The probe sets that measure similar levels of relative gene expression between *G. max*$_{[Peking/PI\ 548402]}$ and *G. max*$_{[PI\ 88788]}$ became the focus of further investigations. In these experiments, combined data from *G. max*$_{[Peking/PI\ 548402]}$ and *G. max*$_{[PI\ 88788]}$ are used to examine gene expression that is common to the two genotypes. The analyses are referred to as combined analyses because they combine the gene expression data of

Table 3 A comparative time course analysis of *G. max*$_{[Peking/PI\ 548402]}$ pericycle, 3, 6 and 9 dpi to *G. max*$_{[PI\ 88788]}$ (baseline) pericycle, 3, 6 and 9 dpi resistant reaction

Probe ID	GenBank ID	Description	Control FC	3 day FC	6 day FC	9 day FC
HIGHER in G. Max[Peking]						
Gma.16558.1.S1_at	CD401715	EMBRYO DEFECTIVE 1374 (EMB1374) transcription regulator	31.79591	21.20895	26.4705	26.49603
GmaAffx.69913.1.A1_at	BU550803	NA	24.21202	5.051458	2.916091	6.453139
Gma.3440.1.S1_s_at	BE820653	Annexin	14.12382	54.12197	92.66703	13.48165
Gma.2527.1.S1_s_at	AW310149	Hydrolase	11.08717	5.22427	2.996417	5.736873
Gma.8075.1.S1_at	BG237495	ARABIDOPSIS THALIANA ROOT FNR 2 oxidoreductase (ATRFNR2)	10.19415	5.114079	5.158075	3.881952
Gma.5213.1.S1_at	BI970096	THIAZOLE REQUIRING (THI1)	10.15316	8.158338	6.591349	5.271578
Gma.2102.1.S1_s_at	BM523392	Disease resistance-responsive family protein/ fibroin-related	9.850742	8.057176	7.452264	14.15474
GmaAffx.51673.1.S1_at	BI892643	Short-chain dehydrogenase/reductase (SDR) family protein	9.722524	2.64891	3.870993	3.53163
Gma.17814.1.S1_at	AW349375	SMALL AND BASIC INTRINSIC PROTEIN 1A (SIP1;1)	8.256599	4.366413	2.854187	8.04231
Gma.4675.1.A1_at	AW309784	NA	7.710598	4.218979	2.518369	3.656552
Gma.6742.1.A1_at	BU544682	NA	5.91864	3.658485	1.933151	6.97982
GmaAffx.65225.1.A1_at	BU544196	NA	5.310171	2.118906	2.690097	2.07855
Gma.9206.1.A1_at	BE658223	DNAJ/HSP40 homolog	5.133189	65.02919	52.75578	24.94265
GmaAffx.92230.1.A1_s_at	CF807955	ARABIDOPSIS THALIANA OSMOTIN 34 (ATOSM34)	5.120276	5.125551	1.916674	8.772659
Gma.6523.1.S1_at	CD416204	COI1 SUPPRESSOR1 (COS1) 6,7-dimethyl-8-ribityllumazine synthase	4.788784	2.881405	2.25572	7.180979
Gma.2048.1.S1_at	BQ273518	Nucleolar protein gar2-related	4.777935	2.453995	1.605651	2.10036
GmaAffx.91617.1.S1_at	CF807342	NA	4.367093	2.467069	3.213129	2.361197
Gma.12929.1.A1_at	BU546100	Aspartyl protease family protein	2.818529	3.993042	1.854135	3.546448
Gma.16111.2.A1_at	BU550402	ACTIN 3 (ACT3)	2.79373	2.501857	2.866219	4.494345
Gma.7795.1.S1_at	AW348257	Rubber elongation factor (REF) family protein	2.729386	3.07138	1.864679	2.939769
Gma.1751.1.S1_at	BE473710	Metalloendopeptidase (MPPBETA)	2.628901	2.164241	1.962112	1.542794
GmaAffx.15031.1.S1_at	BI702292	RESPONSIVE TO DEHYDRATION 19 (RD19) cysteine-type peptidase	2.376732	4.544688	2.310617	5.041949
Gma.3483.1.S1_at	BQ628029	Kelch repeat-containing F-box family protein	2.14176	4.415777	2.121393	4.804158
Gma.2161.1.S1_a_at	CD404355	U6 snRNA-associated Sm-like protein	2.136185	1.547407	1.547049	1.890467
Gma.6474.1.A1_x_at	BI788042	ACCELERATED CELL DEATH 11 (ACD11)	1.899929	2.102296	1.574223	1.937353
LOWER in G. Max[Peking]						
GmaAffx.90343.1.S1_s_at	CF806068	GAST1 PROTEIN HOMOLOG 4 (GASA4)	−2.302606	−5.027036	−6.657755	−3.610013
Gma.2826.1.S1_at	CD397710	TRANSPARENT TESTA 5 (TT5) chalcone isomerase	−5.625007	−10.76999	−14.78268	−12.8567
GmaAffx.68100.1.S1_at	BG508944	Methionine synthase	−6.545762	−11.58697	−22.02279	−18.49992
GmaAffx.69560.1.S1_s_at	BQ628396	Chloroplast 30S ribosomal protein S3	−14.02727	−4.018961	−12.89894	−13.99015
GmaAffx.38387.1.S1_s_at	BM525407	NA	−4.462678	−4.462678	−13.47634	−6.688526

Genes with higher and lower relative levels of gene expression are provided. *FC* Fold change, *PV P* value. The analysis shows suppressed genes. A $\geq|\pm 1.5|$ fold cutoff and $P \leq 0.05$ was used. FDR was set to 12%. The probe set satisfied the criteria set by the differential expression and FDR analyses. Full information for the 4-point time course analysis (Supplemental Table 6) is provided

G. max$_{[Peking/PI\ 548402]}$ and *G. max*$_{[PI\ 88788]}$ at each time point. The analyses result in the identification of probe sets that measure induced or suppressed levels of gene expression at each time point as compared to pericycle and the surrounding cells. The analyses are unlike the previous experiments that were designed to measure relative

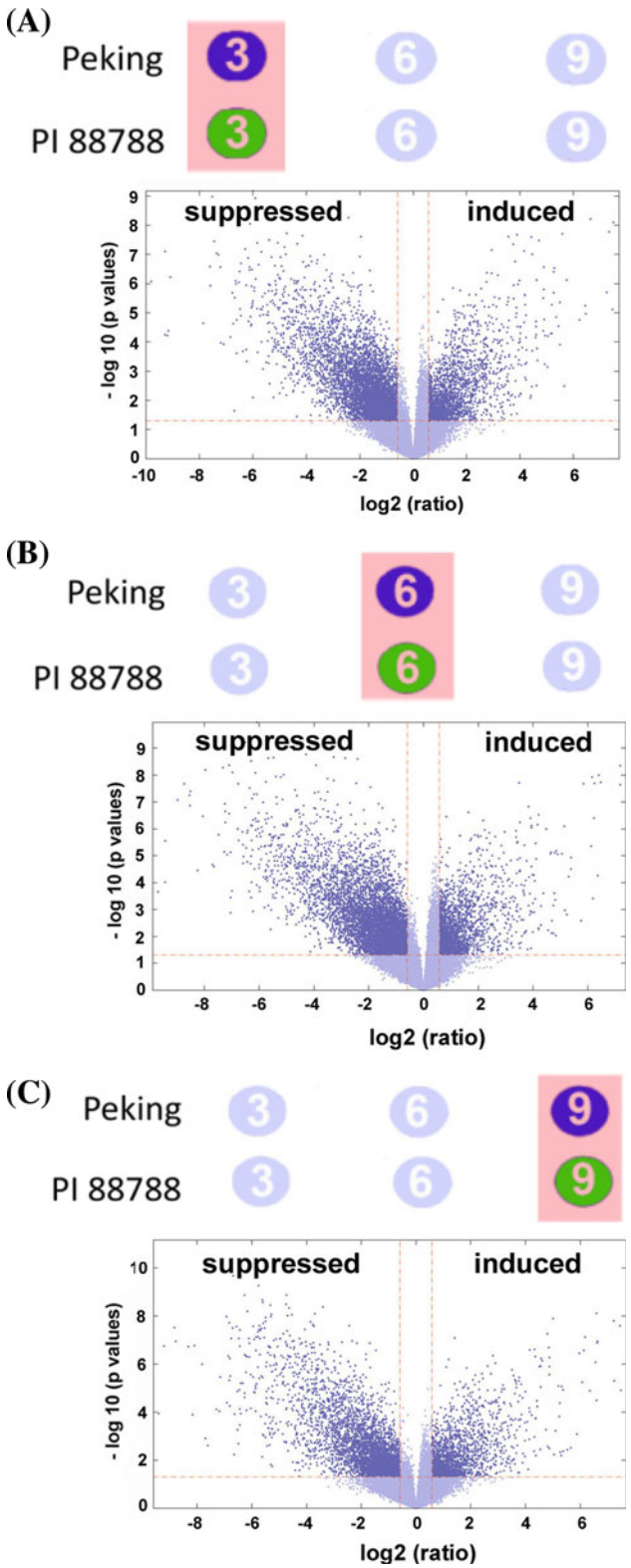

◄ **Fig. 6** Volcano plots comparing differential gene expression of the 3, 6 or 9 $dpi_{[Peking/PI\ 548402\ +\ PI\ 88788]}$ combined syncytium samples to the $pericycle_{[Peking/PI\ 548402\ +\ PI\ 88788]}$ combined sample. The *pink box* depicts the sample types under study. A $\geq|\pm 1.5|$ fold cutoff and $P \leq 0.05$ with a FDR set at 12% was used for the analyses. Induced genes, *dark blue*, *upper right quadrant*. Suppressed genes, *dark blue*, *upper left quadrant*. **a** 3 $dpi_{[Peking/PI\ 548402\ +\ PI\ 88788]}$ combined resistant syncytium sample as compared to the $pericycle_{[Peking\ +\ PI\ 88788]}$ combined sample. **b** 6 $dpi_{[Peking/PI\ 548402\ +\ PI\ 88788]}$ combined syncytium sample as compared to the $pericycle_{[Peking/PI\ 548402\ +\ PI\ 88788]}$ combined sample. **c** 9 $dpi_{[Peking/PI\ 548402\ +\ PI\ 88788]}$ combined syncytium sample as compared to the $pericycle_{[Peking/PI\ 548402\ +\ PI\ 88788]}$ combined sample

expression levels between the two genotypes (Fig. 4). In the combined analyses, all probe sets that measured statistically significant differences in relative levels of gene expression between *G. max*$_{[Peking/PI\ 548402]}$ and *G. max*$_{[PI\ 88788]}$ were eliminated from further analyses. The combined analyses use the 3 replicates from *G. max*$_{[Peking/PI\ 548402]}$ and 3 from *G. max*$_{[PI\ 88788]}$ from each time point, totaling 6 replicates. The combined replicates are used to compare the 3, 6 or 9 $dpi_{[Peking/PI\ 548402\ +\ PI\ 88788]}$ samples to the $pericycle_{[Peking/PI\ 548402\ +\ PI\ 88788]}$ control (Fig. 6).

In the first combined analysis, the 3 $dpi_{[Peking/PI\ 548402\ +\ PI\ 88788]}$ syncytium is compared to $pericycle_{[Peking/PI\ 548402\ +\ PI\ 88788]}$ (Fig. 6a). The analysis identified 1983 probe sets that measure induced levels of gene expression and 4404 probe sets measuring suppressed levels of gene expression in the 3 $dpi_{[Peking/PI\ 548402\ +\ PI\ 88788]}$ syncytium sample (Supplemental Table 7). In the second combined analysis, the 6 $dpi_{[Peking/PI\ 548402\ +\ PI\ 88788]}$ sample is compared to the $pericycle_{[Peking/PI\ 548402\ +\ PI\ 88788]}$ sample (Fig. 6b). The analysis identified 2118 probe sets that measure induced levels of gene expression and 5387 probe sets that measure suppressed levels of gene expression in the 6 $dpi_{[Peking/PI\ 548402\ +\ PI\ 88788]}$ syncytium sample (Supplemental Table 8). In the third combined analysis, the 9 $dpi_{[Peking\ +\ PI\ 88788]}$ sample is compared to the $pericycle_{[Peking/PI\ 548402\ +\ PI\ 88788]}$ sample (Fig. 6c). The analysis identified 2739 probe sets that measure induced levels of gene expression and 1639 probe sets that measure suppressed levels of gene expression in the 9 $dpi_{[Peking/PI\ 548402\ +\ PI\ 88788]}$ syncytium sample (Supplemental Table 9).

The prior combined analyses, examining individual time points, are examined further to identify probe sets consistently measuring induced or suppressed levels of gene expression throughout the infection process. Time course analyses of the combined samples identified probe sets that measure induced or suppressed levels of gene expression across all time points (3, 6 and 9 $dpi_{[Peking/PI\ 548402\ +\ PI\ 88788]}$) as compared to the $pericycle_{[Peking/PI\ 548402\ +\ PI\ 88788]}$ (Fig. 7; Supplemental Table 10). The analysis identified 305 probe sets that measure induced levels of gene expression during the 3, 6 and 9 dpi time points. Probe sets measuring induced gene expression at or greater than an arbitrarily selected cutoff of 20-fold in at least one of the 3 time points and having statistically

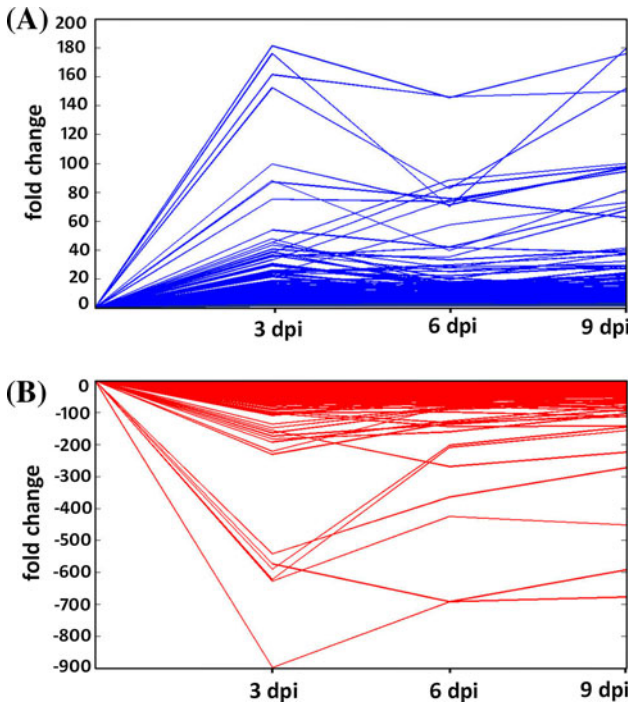

Fig. 7 Line graph depicting genes that are induced or suppressed in syncytium samples at the 3, 6 and 9 dpi time points as compared to pericycle samples in both *G. max*$_{[Peking/PI\ 548402]}$ and *G. max*$_{[PI\ 88788]}$. A $\geq|\pm 1.5|$ fold cutoff and $P \leq 0.05$ with a FDR set at 12% was used for the analyses. **a** Induced genes. **b** Suppressed genes

significant levels of induced gene expression at the other two time points are presented (Table 4). In contrast, there are 720 probe sets that measure suppressed levels of gene expression at all three time points. Probe sets measuring suppressed levels of gene expression of less than an arbitrarily selected cutoff of −50-fold in at least one of three time points are presented (Table 5; Supplemental Table 10).

Discussion

Resistance in plants to pathogens is a complex and multi-faceted process, involving hormones such as jasmonic acid and salicylic acid, resistance proteins (R-genes), small RNAs, enzymatic processes as well as secondary metabolites such as terpenoids and stilbenoids (among many others). The differences in metabolic activity of the cells under pathogen attack are accompanied by subtle but important differences in the cellular architecture at the interface between plants and their parasites. For example, in *Triticum aestivum*, changes in the wheat leaf cuticle are associated with resistance to the Hessian fly, *Mayetiola destructor* (Say) (Kosma et al. 2010). In *G. max*$_{[Peking]}$, cytological changes have also been associated with *H. glycines* infection that include the formation of CWAs (Kim et al. 1987; Kim and Riggs 1992). An understanding of the resistant reaction has been aided by the use of cytological stains such as safranin, a stain that preferentially stains lignin, suberin and cutin. These secondary metabolites have all been shown to be associated with resistance by plants to pathogens. However all of the genes involved in the processes remain to be identified.

In *G. max*, mapping efforts have been published since 1960 (Caldwell et al. 1960; reviewed in Concibido et al. 2004). More recently, sequencing efforts of regions spanning the resistant loci have been performed, resulting in the identification of and subsequent supposition that the genes responsible for *H. glycines* resistance were R-genes of the leucine rich repeat (LRR) class. However, in at least one case, the R-gene proposed to be responsible for the resistance of *G. max* to *H. glycines* a decade ago at the *rhg1* locus does not function in the process (Melito et al. 2010). It is unlikely that the few resistant plant introductions contain all of the genes or have lesions in all of the genes involved in the resistance process. Thus, alternative approaches like the transcriptomic analyses of the syncytium undergoing the different forms of the resistant reaction presented here may help in identifying the genes through their expression patterns. This is an important tool especially if no lesions exist in the genes regulating the process.

The interaction between soybean and the soybean cyst nematode is a very specific reaction with the outcome regulated by both the genotype of the plant and the population of the nematode. Prior analyses have shown that a single *G. max* genotype, *G. max*$_{[Peking/PI\ 548402]}$, responds differently to two distinct populations of *H. glycines* during infection (Klink et al. 2007a, b, 2009a, 2010b). The studies reveal that whole *H. glycines*-infected roots of *G. max*$_{[Peking/PI\ 548402]}$ are undergoing modulations in gene expression activity by 12 h post infection (hpi) as the roots develop a resistant (*H. glycines*$_{[NL1\text{-}RHg/HG\text{-}type\ 7]}$-infected) or a susceptible (*H. glycines*$_{[TN8/HG\text{-}type\ 1.3.6.7]}$-infected) reaction (Klink et al. 2007b). It is known that *G. max*$_{[Peking/PI\ 548402]}$ makes syncytia that are indistinguishable from each other in *H. glycines*$_{[NL1\text{-}RHg/HG\text{-}type\ 7]}$ and *H. glycines*$_{[TN8/HG\text{-}type\ 1.3.6.7]}$ infected roots at 3 dpi (Klink et al. 2007a, b, 2009a, 2010b), consistent with numerous cytological and ultrastructural studies (Endo 1965; Riggs et al. 1973; Acido et al. 1984; Kim et al. 1987). It is unclear what factor(s) underlie the inability of *H. glycines*$_{[NL1\text{-}RHg/HG\text{-}type\ 7]}$ to sustain a susceptible reaction in *G. max*$_{[Peking/PI\ 548402]}$ or *G. max*$_{[PI\ 88788]}$. Complicating the issue is the ability of *H. glycines*$_{[NL1\text{-}RHg/HG\text{-}type\ 7]}$ to successfully infect other soybean genotypes such as the susceptible *G. max*$_{[Kent/PI\ 548586]}$ (Alkharouf et al. 2006), *G. max*$_{[MiniMax/PI\ 643148]}$ (Klink et al. 2008) or *G. max*$_{[Williams\ 82/PI\ 518671]}$ (Klink et al. 2009b). However,

Table 4 Combined analysis-induced genes

Probe ID	GenBank ID	Description	3 day FC	6 day FC	9 day FC
Gma.4837.1.S1_at	BI969343	Nitrate transporter (NTP2)	181.3572	145.4725	175.9298
GmaAffx.92537.1.S1_at	CF808262	Thioredoxin domain 2	175.9624	70.10148	179.7424
GmaAffx.1301.90.S1_s_at	BU764871	CPRD49 protein	161.4081	146.0749	149.7704
Gma.17258.1.S1_s_at	BG509247	Plasma membrane intrinsic polypeptide	152.3878	82.58841	151.862
Gma.17884.1.S1_s_at	BE023599	Thioredoxin domain 2	99.4765	71.36182	97.50129
GmaAffx.33851.1.S1_s_at	BG652918	Plasma membrane intrinsic polypeptide	88.00568	39.70022	81.5681
Gma.3979.1.A1_at	BQ453202	Oxidoreductase	87.12431	75.71694	62.45248
Gma.16908.1.S1_at	CA851713	PLEIOTROPIC DRUG RESISTANCE 7 (ATPDR7/PDR7)	75.18718	73.5342	96.55285
GmaAffx.80899.1.S1_at	AW348263	N/A	53.88037	42.11188	70.05612
Gma.8957.1.A1_at	BU764905	Major latex protein-related	47.88715	15.74441	11.18471
Gma.4359.2.S1_at	BI968877	Thioredoxin domain 2	45.34362	19.66089	37.8791
Gma.5584.4.S1_s_at	BQ610991	N/A	45.278	88.56125	99.81554
Gma.13252.1.S1_at	AW423744	NOD26-LIKE INTRINSIC PROTEIN 4;1	43.53536	27.86329	41.55307
Gma.15653.1.S1_at	BI969594	CPRD49 protein	40.63952	33.25427	39.99826
GmaAffx.73751.1.S1_at	BM522529	N/A	38.84616	14.81812	23.665
GmaAffx.89473.2.S1_s_at	CK605927	N/A	38.46777	84.22387	97.94334
Gma.2091.1.S1_at	AW310549	XYLOGLUCAN ENDOTRANSGLYCOSYLASE 6 (XTR6)	38.24392	25.02714	29.43529
Gma.2133.1.S1_at	AW310071	Alcohol acyl-transferases	36.5949	17.34826	22.66635
GmaAffx.74899.1.S1_at	CA852377	N/A	36.47777	35.29959	67.62322
Gma.8365.1.S1_at	CD396813	ALUMINUM SENSITIVE 3 (ALS3)	35.51154	42.02656	38.02428
GmaAffx.89473.2.A1_x_at	CK605927	N/A	33.28526	75.07749	94.55186
GmaAffx.92561.1.S1_s_at	CF808286	N/A	30.65457	15.39094	20.09656
Gma.5935.2.S1_a_at	AW278477	N/A	30.00026	16.70724	17.58698
Gma.1756.1.S1_at	BF324935	Vacuolar processing enzyme gamma (GAMMA-VPE)	29.66051	17.17768	10.50706
Gma.10827.3.S1_at	AW758966	Oxidoreductase	29.51436	18.3841	20.67453
Gma.5935.1.S1_at	CA852006	N/A	29.35104	14.84596	16.74258
GmaAffx.80180.1.A1_at	AW349390	EPSP synthase	29.23712	16.35677	23.59011
Gma.10854.1.S1_at	CA802334	Nodulin-like protein	26.06708	25.32662	32.33187
Gma.8130.1.S1_at	AI966352	Malate synthase	25.21859	27.49575	27.0197
Gma.2771.1.S1_at	AW309763	N/A	24.77934	11.3021	12.5791
Gma.5507.1.A1_s_at	BM108115	N/A	24.54817	22.31649	29.17702
Gma.3668.1.S1_a_at	AW349263	1-Aminocyclopropane-1-carboxylate oxidase (ACC oxidase)	24.41935	29.84423	36.97905
Gma.3987.1.S1_at	BQ453408	IMP dehydrogenase/GMP reductase	24.37939	11.45596	13.33563
GmaAffx.74127.1.S1_at	AW568912	PLEIOTROPIC DRUG RESISTANCE 6 (ATPDR6/PDR6)	24.18316	29.04658	29.15252
GmaAffx.89473.2.A1_at	CK605927	N/A	23.84398	57.47345	72.94942
Gma.1756.1.S1_x_at	BF324935	Vacuolar processing enzyme gamma (GAMMA-VPE)	22.99967	15.05816	9.772365
Gma.1263.1.S1_at	AY144180	PHOSPHOENOLPYRUVATE CARBOXYLASE KINASE 2 (PPCK2)	21.98572	10.48921	7.622626
Gma.4359.1.S1_a_at	AI794712	Thioredoxin domain 2	21.94326	11.43655	14.28961
Gma.6642.1.A1_at	BE610052	Armadillo/beta-catenin repeat family protein	21.50123	10.42401	8.855311

A comparative analysis of the combined resistance reaction comparing 3, 6 and 9 $dpi_{[Peking/PI\ 548402\ +\ PI\ 88788]}$ to the $pericycle_{[Peking/PI\ 548402\ +\ PI\ 88788]}$ (baseline). *FC* Fold change, *PV P* value; com, combined. A $\geq|\pm 1.5|$ fold cutoff and $P \leq 0.05$ was used. FDR was set to 12%. The probe set satisfied the criteria set by the differential expression and FDR analyses. Full gene lists are Supplemental Table 10

Table 5 Combined analysis-suppressed genes

Probe ID	GenBank ID	Description	3 day FC	6 day FC	9 day FC
GmaAffx.91442.1.S1_at	CF805736	Stress-induced protein SAM22	−897.9834	−692.1131	−591.788
Gma.6999.3.S1_s_at	CF921432	Stress-induced protein SAM22	−627.6774	−425.2879	−452.2152
Gma.6999.2.S1_s_at	X60043	Stress-induced protein SAM22	−622.328	−208.9094	−155.8947
Gma.6999.1.S1_s_at	AF529303	Stress-induced protein SAM22	−590.5102	−202.3408	−145.2682
GmaAffx.91091.1.A1_at	CF806816	OSMOTIN 34 (ATOSM34)	−573.473	−691.8259	−676.8448
GmaAffx.90703.1.A1_at	CF809087	Class III peroxidase	−542.0378	−363.9944	−272.1859
Gma.6999.1.S1_x_at	AF529303	Stress-induced protein SAM22	−230.486	−131.8197	−112.7692
GmaAffx.43551.1.S1_at	AW101224	Epoxide hydrolase	−220.7934	−78.91801	−94.56628
GmaAffx.7738.1.S1_s_at	BE058056	N/A	−191.8086	−126.3119	−77.05466
GmaAffx.90097.1.S1_at	CF805822	ARABIDOPSIS THALIANA EXPANSIN A16 (ATEXPA16)	−182.8408	−159.7812	−102.9616
GmaAffx.671.1.S1_at	CA785167	ARABIDOPSIS THALIANA EXPANSIN A16 (ATEXPA16)	−173.251	−136.7262	−104.0401
Gma.5785.1.S1_at	BI943300	Endo-1,4-beta-glucanase	−163.7475	−91.02507	−71.93401
Gma.8144.1.A1_at	BU548599	Peroxidase	−156.2049	−268.5381	−223.8144
Gma.413.1.S1_at	BQ611370	Peroxidase 12 (PER12)	−147.7885	−86.6731	−54.48467
Gma.4829.1.S1_at	AW309606	Peroxidase	−136.0648	−82.92677	−38.63701
GmaAffx.10710.1.S1_s_at	AW278629	Pathogenesis-related protein PR-1 precursor	−108.9026	−61.13944	−59.67152
Gma.15760.1.S1_at	BE823195	Histone H3	−106.2577	−54.28122	−35.8704
Gma.17993.1.S1_s_at	BQ628525	ATOSM34 (OSMOTIN 34)	−102.6187	−143.6977	−141.4526
GmaAffx.90861.1.S1_at	CF805971	N/A	−100.1445	−97.9008	−110.9905
GmaAffx.65048.1.S1_s_at	BQ628412	N/A	−98.83867	−78.19184	−65.50682
Gma.3604.1.S1_at	AW349604	Caffeoyl-CoA 3-*O*-methyltransferase	−97.15329	−131.8877	−91.56036
Gma.6327.1.S1_s_at	BM731752	Senescence-associated protein	−91.85182	−70.45923	−71.3001
Gma.16709.1.S1_s_at	BQ742929	Cytochrome P450	−90.20964	−70.88486	−67.98326
Gma.1326.1.S1_at	CD397515	Pectate lyase family protein	−87.18268	−57.86263	−51.77156
GmaAffx.31985.1.S1_at	BI320384	*Arabidopsis thaliana* chitinase class IV (ATEP3)	−82.44353	−68.22105	−84.34828
Gma.13110.1.S1_at	CD394837	ARABIDOPSIS THALIANA EXPANSIN A1 (ATEXPA1)	−78.24623	−46.97824	−36.09789
GmaAffx.90390.1.S1_at	CF806115	Peroxidase 12 (PER12)	−76.10898	−63.17044	−45.64938
GmaAffx.42893.1.A1_at	BU549612	Short-chain dehydrogenase/reductase (SDR)	−76.05193	−54.56057	−42.04273
GmaAffx.93392.1.S1_s_at	CF807760	Disease resistance-responsive family protein	−75.12781	−56.15482	−47.10637
Gma.9228.1.S1_at	CD417435	Arabinogalactan-protein	−72.61606	−44.5325	−34.99915
Gma.2523.1.S1_s_at	CA852440	R 14 protein	−71.60612	−91.03295	−61.58156
Gma.15907.1.A1_s_at	CD407154	Leucine-rich repeat protein	−69.31699	−53.50557	−52.53084
Gma.15715.1.S1_at	CD403744	NOD26-like intrinsic protein 1;2 (NIP1;2/NLM2)	−68.95551	−51.05334	−52.08829
Gma.576.1.S1_at	BM732317	Invertase/pectin methylesterase inhibitor	−67.62666	−52.36145	−43.47715
GmaAffx.93214.1.S1_at	CF808939	Cinnamate 4-hydroxylase	−66.4193	−77.81764	−57.90429
Gma.8401.1.A1_at	BU547972	Cytochrome P450, family 71, subfamily B, polypeptide 34 (CYP71B3)	−65.65226	−72.91756	−86.79321
GmaAffx.89772.10.A1_s_at	CK606097	Stress-induced protein SAM22	−64.95094	−46.49229	−80.43811
Gma.2833.1.S1_s_at	AF202731	BASIC CHITINASE (ATHCHIB)	−64.46766	−47.3571	−38.70762
Gma.7436.1.S1_at	BU547698	PLANTACYANIN	−63.56152	−74.54568	−57.79718
GmaAffx.666.1.S1_at	BM143164	Extracellular dermal glycoprotein (EDGP)	−61.81902	−47.06001	−10.94365
GmaAffx.91087.1.S1_s_at	CF806812	Endo-1,4-beta-glucanase	−60.08572	−34.73255	−33.00312
Gma.9164.1.S1_at	CA802402	Histone H4	−56.8739	−32.03909	−26.51658
Gma.4185.1.S1_at	BQ742395	ARABIDOPSIS THALIANA EXPANSIN-LIKE B1 (ATEXLB1)	−56.60563	−48.58276	−40.16978
Gma.413.1.S1_s_at	BQ611370	Peroxidase 12 (PER12)	−55.98323	−41.66081	−29.62947

Table 5 continued

Probe ID	GenBank ID	Description	3 day FC	6 day FC	9 day FC
Gma.7631.1.A1_at	AW309495	Malate dehydrogenase/NADP-MALIC ENZYME 3 (ATNADP-ME3)	−55.34567	−68.28899	−46.8821
Gma.154.1.S1_at	Y10490	Cytochrome P450, family 71, subfamily B, polypeptide 34 ("CYP71B34)	−52.86155	−63.53077	−86.40897
Gma.876.1.S1_at	L78163	Peroxidase	−52.25232	−54.85669	−28.92915
GmaAffx.54524.1.S1_at	BU551371	Caffeoyl-CoA 3-*O*-methyltransferase (CCoAMT)	−50.93016	−28.59014	−21.32015
Gma.4434.1.S1_at	BE659015	ARABIDOPSIS BLUE-COPPER-BINDING PROTEIN (ATBCB)	−50.29084	−47.34821	−43.85539
Gma.3713.1.S1_s_at	BI469834	Trypsin_and_protease_inhibitor_family_protein/ Kunitz_family_protein	−43.4449	−61.40882	−43.33708
Gma.5590.1.S1_a_at	BE822176	3-Deoxy-D-arabino-heptulosonate_7-phosphate_synthase	−33.39936	−54.02632	−44.45494
GmaAffx.75992.1.S1_at	BU548101	N/A	−31.54975	−50.64437	−38.10328

A comparative analysis of the combined resistance reaction comparing 3, 6 and 9 $dpi_{[Peking/PI\ 548402\ +\ PI\ 88788]}$ to the $pericycle_{[Peking/PI\ 548402\ +\ PI\ 88788]}$ (baseline). *FC* Fold change, *PV P* value, *com* combined. A $\geq|\pm 1.5|$ fold cutoff and $P \leq 0.05$ was used. FDR was set to 12%. The probe set satisfied the criteria set by the differential expression and FDR analyses. Full gene lists are Supplemental Table 10

experiments comparing gene expression of syncytia in *G. max*$_{[Peking/PI\ 548402]}$ during resistant (*H. glycines*$_{[NL1\text{-}RHg/HG\text{-}type7]}$-infected) or susceptible (*H. glycines*$_{[TN8/HG\text{-}type\ 1.3.6.7]}$-infected) reactions at 3 dpi reveal modulations in gene activity between the two reaction types (Klink et al. 2007a, 2009a, 2010b).

Experiments have demonstrated that *H. glycines* can alter gene expression in a normally resistant *G. max* genotype to accommodate its infection and pathogenicity (Mahalingham et al. 1999; Klink et al. 2007a, b, 2009a, 2010b). The question remained as to how these different nematode populations are equipped to accomplish a susceptible reaction in an otherwise resistant genotype. Recent transcriptomic experiments examining *H. glycines*$_{[NL1\text{-}RHg/HG\text{-}type\ 7]}$ and *H. glycines*$_{[TN8/HG\text{-}type\ 1.3.6.7]}$ revealed that the two nematode populations were indeed different, even before they infected the roots of *G. max*$_{[Peking/PI\ 548402]}$ (Klink et al. 2009b). Some of these *H. glycines* genes experiencing different levels of gene expression are putative parasitism genes (Klink et al. 2009b). This discovery demonstrated that amplitude differences in putative parasitism genes accompany a compatible reaction as compared to an incompatible reaction. It remains to be demonstrated whether these amplitude differences contribute to a compatible reaction in an otherwise resistant soybean genotype. Differences at the DNA level have been observed for avirulent and virulent *H. glycines* populations as revealed by the use of 454 microbead sequencing (Bekal et al. 2008). The work reinforces evidence provided by transcriptomic analyses (Klink et al. 2009b) that genetic differences are present between avirulent and virulent *H. glycines* populations.

Studies have examined modulations in gene activity in various resistant *G. max* genotypes during infection by *H. glycines* race 3 (Mahalingham et al. 1999). Mahalingham et al. (1999) examined protein expression during the resistant reaction in three different *G. max* genotypes exhibiting resistance to *H. glycines*. The *G. max* genotypes used in the analysis were *G. max*$_{[Peking]}$, *G. max*$_{[PI\ 88788]}$ and *G. max*$_{[PI\ 437654]}$. Thus, the study relates well to the work presented here. The study investigated polygalacturonase (PG) and polygalacturonase inhibitor protein (PGIP) expression in roots infected with race 3 and race 14. The race 3 used in Mahalingham et al. (1999) study functions in a similar way in their *G. max*$_{[Peking]}$ and *G. max*$_{[PI\ 88788]}$ genotypes as the *H. glycines* HG-type 7 population used in the analyses presented here. In those studies, race 3 would elicit a resistant reaction in *G. max*$_{[Peking]}$ and *G. max*$_{[PI\ 437654]}$ and *G. max*$_{[PI\ 88788]}$. Race 14 would elicit a resistant reaction in *G. max*$_{[PI\ 88788]}$ and *G. max*$_{[PI\ 437654]}$ and a susceptible reaction in *G. max*$_{[Peking]}$. The studies demonstrated modulations in PG and PGIP proteins with amplified levels of PG in *G. max*$_{[Peking]}$ as compared to *G. max*$_{[PI\ 88788]}$ and *G. max*$_{[PI\ 437654]}$ (Mahalingham et al. 1999). While the induced and amplified levels were found in the susceptible reaction, it demonstrated that both induced and amplified expression do occur in different *G. max* genotypes infected with the same *H. glycines* population (Mahalingham et al. 1999) which is exactly what we observed in our genomics-based analyses.

Genotype-specific modulations in gene expression at the site of the resistant reaction

A gap in knowledge from those experiments is how a single *H. glycines* population (i.e., NL1-RHg/HG-type 7)

can elicit resistant reactions that are completely different at the cellular level in two different *G. max* genotypes. The advantage of procedures such as the LCM methodology is that the cells of interest can be purified to the exclusion of those not involved in the process. Subsequent bioinformatics analyses have allowed for the determination of whether the vast differences in cytology observed for the different resistant reactions at the site of infection for the *G. max*$_{[Peking/PI\ 548402]}$-type and *G. max*$_{[PI\ 88788]}$-type reactions are accompanied by diverse transcriptomic patterns. The analyses have also determined whether those differences in gene expression are imprinted into the root cells prior to infection or only occur after nematode infection. Alternatively, it is possible that such experiments would reveal only conserved patterns of expression that are accompanied by specific modulations in gene expression characteristic of each genotype that are occurring during the respective resistant reactions of *G. max*$_{[Peking/PI\ 548402]}$ and *G. max*$_{[PI\ 88788]}$. The analysis presented here fills that gap in knowledge by examining resistant reactions in action in *G. max*$_{[Peking/PI\ 548402]}$ and *G. max*$_{[PI\ 88788]}$ to *H. glycines*$_{[NL1\text{-}RHg/HG\text{-}type\ 7]}$, locally at the syncytium. Many of the identified genes are not discussed here because they have been discussed in the individual analyses of *G. max*$_{[Peking/PI\ 548402]}$ (Klink et al. 2007a, 2009a) and *G. max*$_{[PI\ 88788]}$ (Klink et al. 2010a). We note that all genes identified in these analyses, while experiencing differences in expression level, may not relate to the resistant reaction in any way.

Gene expression in pericycle cells of *G. max*$_{[Peking]}$ is different to *G. max*$_{[PI\ 88788]}$ prior to the introduction of *H. glycines*$_{[NL1\text{-}RHg/HG\text{-}type\ 7]}$ to the roots

The first set of analyses compare *G. max*$_{[Peking/PI\ 548402]}$ to *G. max*$_{[PI\ 88788]}$ pericycle and surrounding cells, revealing differences in gene expression are present. The result demonstrates it is possible that determinants involved in resistance could be imprinted within the pericycle and surrounding cells (i.e., the nurse cell initials) prior to infection. One gene that experiences the largest difference in relative gene expression in *G. max*$_{[Peking/PI\ 548402]}$ pericycle is DEA1. The *G. max* DEA1 cDNA (CA850542) was originally isolated from *G. max*$_{[Peking/PI\ 548402]}$ roots infected with *H. glycines*$_{[NL1\text{-}RHg/HG\text{-}type\ 7]}$) at 2 and 4 dpi (N. W. Alkharouf and B. F. Matthews, unpublished data). In tomato, DEA1 exhibits organ-specific expression. DEA1 is highly expressed in roots, stems, and leaves (Weyman et al. 2006a). The DEA1 gene is induced by arachidonic acid (AA). AA is a polyunsaturated fatty acid molecule that is produced by various pathogens (i.e., *Phytopthora infestans*) and is known to trigger programmed cell death (PCD). Cell death has been observed in the syncytia of *G. max*$_{[Peking/PI\ 548402]}$ (Kim and Riggs 1992). In other plant-pathogen interactions, AA is shown to be released from germinating *P. infestans* spores (Ricker and Bostock 1992) and can mimic the PCD response (Bostock et al. 1981; Bostock et al. 1986). The DEA1 primary amino acid sequence has a conserved, shared domain found in the eight-cysteine motif superfamily of protease inhibitors. The domain is also found in proteins such as alpha-amylase inhibitors, lipid transfer proteins and seed storage proteins (Weyman et al. 2006a). Reporter experiments involving normal protoplasts and protoplasts undergoing plasmolysis show that DEA1 is associated with the cell membrane (Weyman et al. 2006a). More recent experiments show that expression of DEA1 in a heterologous yeast system protects the yeast from freezing death (Weyman et al. 2006b). It may be that *G. max* homolog of DEA1 performs a role in the defense response at the site of infection. It may explain why *G. max*$_{[Peking/PI\ 548402]}$ experiences rapid degradation of the syncytium during its resistance reaction while *G. max*$_{[PI\ 88788]}$ experiences a prolonged localized response at the syncytium. The identification of *Gm*-DEA1 is consistent with anatomical studies revealing that nuclei degrade in all forms of the resistant reaction. The process initiates by the formation of masses of chromatin that later scatter and deteriorates within the degenerating cytoplasm (Kim and Riggs 1992). The observation of higher levels of *Gm*-DEA1in *G. max*$_{[Peking/PI\ 548402]}$ earlier than what is found in *G. max*$_{[PI\ 88788]}$ is consistent with its more rapid appearance of the resistance reaction. AA, functioning upstream of jasmonate signaling (Blée 2002) may provide a way to amplify the signal leading to the rapid and potent resistant reaction of *G. max*$_{[Peking/PI\ 548402]}$ and pathway, linking knowledge of the involvement of jasmonate signaling in the resistance of plants to parasitic nematodes (Gao et al. 2008).

Numerous other genes involved in defense and signaling were also identified in pericycle and surrounding cell samples isolated from roots that were not yet exposed to *H. glycines*$_{[NL1\text{-}RHg/HG\text{-}type\ 7]}$. The identification of EMB1374 (CD401715) implicates MAP-kinase signaling cascades that could be more active in *G. max*$_{[Peking/PI\ 548402]}$ than in *G. max*$_{[PI\ 88788]}$ even before infection occurs. A probe set with homology to the *A. thaliana* gene At4g26500 (NP 194380) measures higher relative gene expression levels in *G. max*$_{[Peking/PI\ 548402]}$ pericycle control samples as well as syncytia microdissected from 3, 6 and 9 dpi roots. The CD401715 expressed sequence tag (EST) has homology to a gene known as embryo defective 1374 (EMB1374). EMB1374 is also known as ARABIDOPSIS THALIANA SULFUR E, ATSUFE, CHLOROPLAST SULFUR E, CPSUFE and SULFUR E 1, SUFE1. The EMB1374 mutant was originally isolated in a genetic

screen in *A. thaliana* for mutants that were embryo defective (Tzafrir et al. 2001; McElver et al. 2001). In *A. thaliana*, EMB1374 both interacts with and activates the cysteine desulfurases, AtSufS in plastids and AtNifS1 in mitochondria. Each of these activations is vital during embryogenesis. Dual localization of the EMB1374 protein occurs in mitochondria and chloroplasts. EMB1374 is involved in Fe–S cluster biogenesis in both mitochondria and plastids. Little was known about how the gene works in plants until recent experiments in *A. thaliana* demonstrated that EMB1374 interacts with mitogen-activated protein kinase-1 (MPK1) and MPK16 (Popescu et al. 2008). Thus, EMB1374 may play a central role in a variety of important signaling cascades within plant cells. For example, MPK1 alone has been shown to be phosphorylated by the MPK-activating kinases (MKKs) 1, 3, 7 and 10 (Popescu et al. 2008). MPK1 phoshorylates the downstream transcription factor targets WRKY40 and WRKY62 (Popescu et al. 2008). WRKY genes are known to play important roles in developmental processes, defense responses against pathogens and senescence (Eulgem and Somssich 2007). Thus, the analysis identified genes that are present in higher levels in pericycle cells. However the differences in amplitude of some of those genes extended throughout the resistant reaction in *G. max*$_{[Peking/PI\ 548402]}$. The observation demonstrates that the soybean genotypes are fundamentally different in the cells that are involved in the resistant reaction. Some differences are observed prior to the association of nematodes with the root while some of those differences are limited to the period of infection and some exhibit differences in expression that are constitutive.

Pathway analyses reveal amplified levels of genes involved in defense in the rapid and potent resistant reaction of *G. max*$_{[Peking/PI\ 548402]}$ as compared to *G. max*$_{[PI\ 88788]}$

Customized pathway analyses tools have been developed and used to obtain a better understanding of genes having homology to those with known function. The work provides a broader understanding of gene expression during the respective resistant reactions. However, it is noted that pathway analyses are done to the exclusion of many highly induced/suppressed amplified/attenuated genes that may be important to the resistant reaction. The initial analyses first compared both *G. max*$_{[Peking/PI\ 548402]}$ and *G. max*$_{[PI\ 88788]}$ to their respective pericycle cells. The analyses determined induced levels of genes pertaining to important aspects of defense or applicable to defense such as brassinosteroid signaling pathway (Nakashita et al. 2003; He et al. 2007; Chinchilla et al. 2007; Heese et al. 2007; Lu et al. 2010), some components of the fatty acid biosynthesis pathway (Kachroo et al. 2003, 2008; Chandra-Shekara et al. 2007; Reina-Pinto et al. 2009), glycolysis (Scheideler et al. 2002; Colebatch et al. 2002), components of the phenylpropanoid biosynthesis pathway (Cole 1984; Leszczynski et al. 1989; Edens et al. 1995; Wang et al. 2006) and ubiquinone and terpenoid-quinone biosynthesis pathways in the *G. max*$_{[Peking/PI\ 548402]}$ and *G. max*$_{[PI\ 88788]}$ genotypes.

Some of the genes presented here were identified in prior analyses of *G. max*$_{[Peking/PI\ 548402]}$ (Klink et al. 2009a) and *G. max*$_{[PI\ 88788]}$ (Klink et al. 2010a). In contrast to the previous experiments, the analyses presented here determined whether certain pathways were both induced and amplified or suppressed and attenuated in their expression in one genotype in comparison to another. The analyses identified the induced and amplified nature of the brassinosteroid pathway in *G. max*$_{[Peking/PI\ 548402]}$ as compared to *G. max*$_{[PI\ 88788]}$ at 3 dpi (Fig. 5a–c). Similar analyses for the 6 and 9 dpi time points allowed for the identification of other gene pathways that were amplified in *G. max*$_{[Peking/PI\ 548402]}$ as compared to *G. max*$_{[PI\ 88788]}$. Of note, the brassinosteroid pathway while still induced as compared to pericycle and surrounding cells, experiences suppression and attenuation in *G. max*$_{[Peking/PI\ 548402]}$ as compared to *G. max*$_{[PI\ 88788]}$ at the 6 and 9 dpi time points. Other pathway analyses identified the biosynthesis of benzoxazinoids (Cambier et al. 2001; Morant et al. 2008; Sasai et al. 2009), glycosphingolipids (Brodersen et al. 2002), and stilbenoid biosynthesis (Sobolev et al. 2010) to be induced and amplified in *G. max*$_{[Peking/PI\ 548402]}$ as compared to *G. max*$_{[PI\ 88788]}$. These pathways are important in defense of plants to pathogens, revealing important modes of defense that may be employed more efficiently by *G. max*$_{[Peking/PI\ 548402]}$ than *G. max*$_{[PI\ 88788]}$.

Conclusion

It is highly likely that the resistance loci that have been mapped using the various soybean genotypes do not represent all of the genes involved in the process. Therefore, the mapped genes are an underestimate of the genes actually involved in the process. The analysis here employs an alternative strategy to identify genes that may be involved in the process for which no genetic lesions exist. The analysis presented here directly compares nematode feeding sites of the two major and different forms of the resistant reaction, *G. max*$_{[Peking/PI\ 548402]}$ (*G. max*$_{[Peking]}$-type) and *G. max*$_{[PI\ 88788]}$ (*G. max*$_{[PI\ 88788]}$-type). Specifically, the analyses explore the resistance processes of *G. max*$_{[Peking/PI\ 548402]}$ and *G. max*$_{[PI\ 88788]}$, the archetypal sources of nearly all of the resistance germplasm currently used in commercial production for resistance to *H. glycines* (Concibido et al. 2004; Colgrove and Niblack 2008). The resistant reaction, divided here into parasitism and

resistance phases, allowed for a variety of comparative analyses to be performed that reveal gene expression that is unique to the two reaction types at the two phases of the resistant reaction. An aim of the gene expression experiments was to identify induced/amplified or suppressed/attenuated genes in each genotype during their respective resistant reactions. That objective was met. The expression analyses also identify genes that are common to *G. max*$_{[Peking/PI\ 548402]}$ and *G. max*$_{[PI\ 88788]}$ that possibly relate to generalized features of the resistance process. The common gene expression features between the *G. max*$_{[Peking/PI\ 548402]}$ and *G. max*$_{[PI\ 88788]}$ reactions indicate that there is a conserved gene expression mechanism between the two reaction types. In cross-comparisons of the *G. max*$_{[Peking/PI\ 548402]}$ to the *G. max*$_{[PI\ 88788]}$ resistant reaction types, the analyses identify a subset of genes that have induced and amplified levels of gene expression in either genotype at specific time points as well as those with differences throughout the resistant reaction. The genes identified in this and other related analyses (Klink et al. 2009a, 2010a) may actually associate with resistance in the *G. max*$_{[Peking/PI\ 548402]}$ and *G. max*$_{[PI\ 88788]}$ reaction types, respectively. In some cases, these genes are found to have very large differences in relative amounts of gene expression. These genes may be a useful resource for association mapping of resistance genes found uniquely to *G. max*$_{[Peking/PI\ 548402]}$ and *G. max*$_{[PI\ 88788]}$. This is an important point because for decades it has been very difficult to identify the actual resistance genes not only because of the highly duplicated nature of the soybean genome, but because of localized duplications and deletions in and around resistance gene loci (Melito et al. 2010). The analyses demonstrate the value of using microarrays for related soybean genotypes undergoing nematode infection. Such analyses could be expanded to investigations of near isogenic lines (NILs) or recombinant inbred lines (RILs) for identifying candidate resistance genes. However, to determine the gene expression programs underlying the *G. max*$_{[Peking/PI\ 548402]}$ and *G. max*$_{[PI\ 88788]}$ forms of the resistant reaction, it may be more appropriate to use the same nematode population to obtain each resistant reaction and cross compare them to their respective susceptible reactions by using a different nematode population (Klink et al. 2007a, 2009a, 2010b). In doing so, genotype-based differences that affect gene expression even in NILs and RILs are altogether avoided. The use of a high-throughput-Gateway® compatible transformation system designed specifically to investigate this system should aid in the identification of gene function during this important host–parasite interaction (Klink et al. 2009c).

Acknowledgments VPK is a recipient of the Research Initiation Program Grant at Mississippi State University and thankfully acknowledges support provided by the Mississippi Soybean Promotion Board. The authors thank Dr. David Munroe, Nina Bubunenko and Nicole Lum at the Laboratory of Molecular Technology, SAIC-Frederick, National Cancer Institute at Frederick, Frederick, Maryland 21701, USA for the Affymetrix® soybean GeneChip® array hybridizations and data acquisition. Dr. Gary Lawrence Department of Biochemistry, Molecular Biology, Entomology and Plant Pathology, Mississippi State University provided helpful insight into the analysis of the resistance responses of *G. max*$_{[Peking/PI\ 548402]}$ and *G. max*$_{[PI\ 88788]}$.

References

Abad P, Gouzy J, Aury JM, Castagnone-Sereno P, Danchin EG, Deleury E, Perfus-Barbeoch L, Anthouard V, Artiguenave F, Blok VC, Caillaud MC, Coutinho PM, Dasilva C, De Luca F, Deau F, Esquibet M, Flutre T, Goldstone JV, Hamamouch N, Hewezi T, Jaillon O, Jubin C, Leonetti P, Magliano M, Maier TR, Markov GV, McVeigh P, Pesole G, Poulain J, Robinson-Rechavi M, Sallet E, Ségurens B, Steinbach D, Tytgat T, Ugarte E, van Ghelder C, Veronico P, Baum TJ, Blaxter M, Bleve-Zacheo T, Davis EL, Ewbank JJ, Favery B, Grenier E, Henrissat B, Jones JT, Laudet V, Maule AG, Quesneville H, Rosso MN, Schiex T, Smant G, Weissenbach J, Wincker P (2008) Genome sequence of the metazoan plant-parasitic nematode Meloidogyne incognita. Nat Biotechnol 26:909–915

Acido JR, Dropkin VH, Luedders VD (1984) Nematode population attrition and histopathology of *Heterodera glycines-Soybean* associations. J Nematol 16:48–57

Aist JR (1976) Papillae and related wound plugs of plant cells. Annu Rev Phytopathol 14:145–163

Alkharouf NW, Klink VP, Chouikha IB, Beard HS, MacDonald MH, Meyer S, Knap HT, Khan R, Matthews BF (2006) Timecourse microarray analyses reveals global changes in gene expression of susceptible *Glycine max* (soybean) roots during infection by *Heterodera glycines* (soybean cyst nematode). Planta 224: 838–852

Altschul SF, Madden TL, Schaffer AA, Zhang J, Zhang Z, Miller W, Lipman DJ (1997) Gapped BLAST and PSI-BLAST: a new generation of protein database search programs. Nucleic Acids Res 25:3389–3402

Asano T, Masumura T, Kusano H, Kikuchi S, Kurita A, Shimada H, Kadowaki K (2002) Construction of a specialized cDNA library from plant cells isolated by laser capture microdissection: toward comprehensive analysis of the genes expressed in the rice phloem. Plant J 32:401–408

Bekal S, Craig JP, Hudson ME, Niblack TL, Domier LL, Lambert KN (2008) Genomic DNA sequence comparison between two inbred soybean cyst nematode biotypes facilitated by massively parallel 454 micro-bead sequencing. Mol Genet Genomics 279:535–543

Blée E (2002) Impact of phyto-oxylipins in plant defense. Trends Plant Sci 7:315–322

Bostock RM, Kuc J, Laine RA (1981) Eicosapentaenoic and arachidonic acids from *Phytophthora infestans* elicit fungitoxic sesquiterpenes in the potato. Science 212:67–69

Bostock RM, Schaeffer DA, Hammerschmidt R (1986) Comparison of elicitor activities of arachidonic acid, fatty acids and glucans from *Phytopthora infestans* in hypersensitivity expression in potato tuber. Physiol Mol Plant Pathol 29:349–360

Brodersen P, Petersen M, Pike HM, Olszak B, Skov S, Odum N, Jørgensen LB, Brown RE, Mundy J (2002) Knockout of Arabidopsis accelerated-cell-death11 encoding a sphingosine transfer protein causes activation of programmed cell death and defense. Genes Dev 16:490–502

Cai D, Kleine M, Kifle S, Hans-Joachim H, Sandal NN, Marcker KA, Klein-Lankhorst RM, Salentijn EMJ, Lange W, Stiekema WJ, Wyss U, Grundler FMW, Jung C (1997) Positional cloning of a gene for nematode resistance in sugar beet. Science 275:832–834

Caldwell BE, Brim CA, Ross JP (1960) Inheritance of resistance of soybeans to the soybean cyst nematode, *Heterodera glycines*. Agron J 52:635–636

Cambier V, Hance T, De Hoffmann E (2001) Effects of 1,4-benzoxazin-3-one derivatives from maize on survival and fecundity of Metopolophium dirhodum (Walker) on artificial diet. J Chem Ecol 27:359–370

Chandra-Shekara AC, Venugopal SC, Barman SR, Kachroo A, Kachroo P (2007) Plastidial fatty acid levels regulate resistance gene-dependent defense signaling in Arabidopsis. Proc Natl Acad Sci USA 104:7277–7282

Chinchilla D, Zipfel C, Robatzek S, Kemmerling B, Nürnberger T, Jones JD, Felix G, Boller T (2007) A flagellin-induced complex of the receptor FLS2 and BAK1 initiates plant defence. Nature 448:497–500

Cole RA (1984) Phenolic acids associated with the resistance of lettuce cultivars to the lettuce root aphid. Ann Appl Biol 105:129–145

Colebatch G, Kloska S, Trevaskis B, Freund S, Altmann T, Udvardi MK (2002) Novel aspects of symbiotic nitrogen fixation uncovered by transcript profiling with cDNA arrays. Mol Plant Microbe Interact 15411–15420

Colgrove AL, Niblack TL (2008) Correlation of female indices from virulence assays on inbred lines and field populations of *Heterodera glycines*. J Nematol 40:39–45

Concibido VC, Diers BW, Arelli PR (2004) A decade of QTL mapping for cyst nematode resistance in soybean. Crop Sci 44:1121–1131

Edens RM, Anand SC, Bolla RI (1995) Enzymes of the phenylpropanoid pathway in soybean infected with *Meloiodiogyne incognita* or *Heterodera glycines*. J Nematol 27:292–303

Emmert-Buck MR, Bonner RF, Smith PD, Chuaqui RF, Zhuang Z, Goldstein SR, Weiss RA, Liotta LA (1996) Laser capture microdissection. Science 274:998–1001

Endo BY (1964) Penetration and development of *Heterodera glycines* in soybean roots and related and related anatomical changes. Phytopathology 54:79–88

Endo BY (1965) Histological responses of resistant and susceptible soybean varieties, and backcross progeny to entry development of *Heterodera glycines*. Phytopathology 55:375–381

Endo BY (1991) Ultrastructure of initial responses of resistant and susceptible soybean roots to infection by *Heterodera glycines*. Rev Nematol 14:73–94

Eulgem T, Somssich IE (2007) Networks of WRKY transcription factors in defense signaling. Curr Opin Plant Biol 10:366–371

Gao X, Starr J, Göbel C, Engelberth J, Feussner I, Tumlinson J, Kolomiets M (2008) Maize 9-lipoxygenase ZmLOX3 controls development, root-specific expression of defense genes, and resistance to root-knot nematodes. MPMI 21:98–109

Glover KD, Wang D, Arelli PR, Carlson SR, Cianzio SR, Diers BW (2004) Near isogenic lines confirm a soybean cyst nematode resistance gene from PI 88788 on linkage group. J Crop Sci 44:936–941

Golden AM, Epps JM, Riggs RD, Duclos LA, Fox JA, Bernard RL (1970) Terminology and identity of infraspecific forms of the soybean cyst nematode (*Heterodera glycines*). Plant Dis Rep 54:544–546

Halbrendt J, Lewis S, Shipe E (1992) A technique for evaluating *Heterodera glycines* development in susceptible and resistant soybean. J Nematol 24:84–91

Hardham AR, Takemoto D, White RG (2008) Rapid and dynamic subcellular reorganization following mechanical stimulation of Arabidopsis epidermal cells mimics responses to fungal and oomycete attack. BMC Plant Biol 8:63

Hartwig EE, Epps JM (1978) Registration of Bedford soybeans. Crop Sci 18:915

He K, Gou X, Yuan T, Lin H, Asami T, Yoshida S, Russell SD, Li J (2007) BAK1 and BKK1 regulate brassinosteroid-dependent growth and brassinosteroid-independent cell-death pathways. Curr Biol 17:1109–1115

Heese A, Hann DR, Gimenez-Ibanez S, Jones AM, He K, Li J, Schroeder JI, Peck SC, Rathjen JP (2007) The receptor-like kinase SERK3/BAK1 is a central regulator of innate immunity in plants. Proc Natl Acad Sci USA 104:12217–12222

Isenberg G, Bielser W, Meier-Ruge W, Remy E (1976) Cell surgery by laser micro-dissection: a preparative method. J Microsc 107: 19–24

Jones DA, Thomas CM, Hammond-Kosack KE, Balint-Kurti PJ, Jones JD (1994) Isolation of the tomato Cf-9 gene for resistance to Cladosporium fulvum by transposon tagging. Science 266: 789–793

Kachroo A, Lapchyk L, Fukushige H, Hildebrand D, Klessig D, Kachroo P (2003) Plastidial fatty acid signaling modulates salicylic acid- and jasmonic acid-mediated defense pathways in the Arabidopsis ssi2 mutant. Plant Cell 15:2952–2965

Kachroo A, Fu DQ, Havens W, Navarre D, Kachroo P, Ghabrial SA (2008) An oleic acid-mediated pathway induces constitutive defense signaling and enhanced resistance to multiple pathogens in soybean. Mol Plant Microbe Interact 21:564–575

Kim KS, Riggs RD (1992) Cytopathological reactions of resistant soybean plants to nematode invasion. In: Wrather JA, Riggs RD (eds) Biology and management of the soybean cyst nematode. APS Press, St. Paul, pp 157–168

Kim YH, Riggs RD, Kim KS (1987) Structural changes associated with resistance of soybean to *Heterodera glycines*. J Nematol 19:177–187

Klink VP, MacDonald M, Alkharouf N, Matthews BF (2005) Laser capture microdissection (LCM) and expression analyses of *Glycine max* (soybean) syncytium containing root regions formed by the plant pathogen *Heterodera glycines* (soybean cyst nematode). Plant Mol Biol 59:969–983

Klink VP, Overall CC, Alkharouf N, MacDonald MH, Matthews BF (2007a) Laser capture microdissection (LCM) and comparative microarray expression analysis of syncytial cells isolated from incompatible and compatible soybean roots infected by soybean cyst nematode (*Heterodera glycines*). Planta 226:1389–1409

Klink VP, Overall CC, Alkharouf N, MacDonald MH, Matthews BF (2007b) A comparative microarray analysis of an incompatible and compatible disease response by soybean (*Glycine max*) to soybean cyst nematode (*Heterodera glycines*) infection. Planta 226:1423–1447

Klink VP, MacDonald MH, Martins VE, Park S-C, Kim K-H, Baek S-H, Matthews BF (2008) MiniMax, a new diminutive *Glycine max* variety, with a rapid life cycle, embryogenic potential and transformation capabilities. Plant Cell Tissue Organ Cult 92: 183–195

Klink VP, Hosseini P, Matsye P, Alkharouf N, Matthews BF (2009a) A gene expression analysis of syncytia laser microdissected from the roots of the *Glycine max* (soybean) genotype PI 548402 (Peking) undergoing a resistant reaction after infection by *Heterodera glycines* (soybean cyst nematode). Plant Mol Biol 71:525–567

Klink VP, Hosseini P, MacDonald MH, Alkharouf N, Matthews BF (2009b) Population-specific gene expression in the plant pathogenic nematode *Heterodera glycines* exists prior to infection and during the onset of a resistant or susceptible reaction in the roots of the *Glycine max* genotype Peking. BMC Genomics 10:111

Klink VP, Kim K-H, Martins VE, MacDonald MH, Beard HS, Alkharouf NW, Park S-C, Matthews BF (2009c) A correlation between host-mediated expression of parasite genes as tandem inverted repeats and abrogation of the formation of female *Heterodera glycines* cysts during infection of *Glycine max*. Planta 230:53–71

Klink VP, Hosseini P, Matsye P, Alkharouf N, Matthews BF (2010a) Syncytium gene expression in *Glycine max*$_{[PI\ 88788]}$ roots undergoing a resistant reaction to the parasitic nematode *Heterodera glycines*. Plant Physiol Biochem 48:176–193

Klink VP, Overall CC, Alkharouf N, MacDonald MH, Matthews BF (2010b) Microarray detection calls as a means to compare transcripts expressed within syncytial cells isolated from incompatible and compatible soybean (*Glycine max*) roots infected by the soybean cyst nematode (*Heterodera glycines*). J Biomed Biotechnol 2010:491217 (1–30)

Kosma DK, Nemacheck JA, Jenks MA, Williams CE (2010) Changes in properties of wheat leaf cuticle during interactions with Hessian fly. Plant J 63:31–43

Lauritis JA, Rebois R, Graney LS (1983) Development of *Heterodera glycines* Ichinohe on soybean, *Glycine max* (L.) Merr., under gnotobiotic conditions. J Nematol 15:272–280

Leszczynski B, Wright LC, Bakowski T (1989) Effect of secondary plant substances on winter wheat resistance to grain aphid. Entomol Exp Appl 52:135–139

Lu D, Wu S, Gao X, Zhang Y, Shan L, He P (2010) A receptor-like cytoplasmic kinase, BIK1, associates with a flagellin receptor complex to initiate plant innate immunity. Proc Natl Acad Sci USA 107:496–501

Mahalingham R, Skorupska HT (1996) Cytological expression of early response to infection by *Heterodera glycines* Ichinohe in resistant PI 437654 soybean. Genome 39:986–998

Mahalingham R, Wang G, Knap HT (1999) Polygalacturonase and polygalacturonase inhibitor protein: gene isolation and transcription in *Glycine max–Heterodera glycines* interactions. Mol Plant Microbe Interact 12:490–498

Matson AL, Williams LF (1965) Evidence of a fourth gene for resistance to the soybean cyst nematode. Crop Sci 5:477

McElver J, Tzafrir I, Aux G, Rogers R, Ashby C, Smith K, Thomas C, Schetter A, Zhou Q, Cushman MA, Tossberg J, Nickle T, Levin JZ, Law M, Meinke D, Patton D (2001) Insertional mutagenesis of genes required for seed development in *Arabidopsis thaliana*. Genetics 159:1751–1763

Meier-Ruge W, Bielser W, Remy E, Hillenkamp F, Nitsche R, Unsold R (1976) The laser in the Lowry technique for microdissection of freeze-dried tissue slices. Histochem J 8:387–401

Melito S, Heuberger AL, Cook D, Diers BW, MacGuidwin AE, Bent AF (2010) A nematode demographics assay in transgenic roots reveals no significant impacts of the Rhg1locus LRR-kinase on soybean cyst nematode resistance. BMC Plant Biol 10:104

Milligan SB, Bodeau J, Yaghoobi J, Kaloshian I, Zabel P, Williamson VM (1998) The root knot nematode resistance gene Mi from tomato is a member of the leucine zipper, nucleotide binding, leucine-rich repeat family of plant genes. Plant Cell 10:1307–1319

Morant AV, Jørgensen K, Jørgensen C, Paquette SM, Sánchez-Pérez R, Møller BL, Bak S (2008) Beta-glucosidases as detonators of plant chemical defense. Phytochemistry 69:1795–1813

Nakashita H, Yasuda M, Nitta T, Asami T, Fujioka S, Arai Y, Sekimata K, Takatsuto S, Yamaguchi I, Yoshida S (2003) Brassinosteroid functions in a broad range of disease resistance in tobacco and rice. Plant J 33:887–898

Niblack TL, Arelli PR, Noel GR, Opperman CH, Orf JH, Schmitt DP, Shannon JG, Tylka GL (2002) A revised classification scheme for genetically diverse populations of *Heterodera glycines*. J Nematol 34:279–288

Popescu SC, Popescu GV, Bachan S, Zhang Z, Gerstein M, Snyder M, Dinesh-Kumar SP (2008) MAPK target networks in *Arabidopsis thaliana* revealed using functional protein microarrays. Genes Dev 23:80–92

Rao-Arelli AP (1994) Inheritance of resistance to *Heterodera glycines* race 3 in soybean accessions. Plant Dis 78:898–900

Reina-Pinto JJ, Voisin D, Kurdyukov S, Faust A, Haslam RP, Michaelson LV, Efremova N, Franke B, Schreiber L, Napier JA, Yephremov A (2009) Misexpression of FATTY ACID ELONGATION1 in the Arabidopsis epidermis induces cell death and suggests a critical role for phospholipase A2 in this process. Plant Cell 21:1252–1272

Ricker KE, Bostock RM (1992) Evidence for release of the elicitor arachidonic acid and its metabolites from sporangia of *Phytophthora infestans* during infection of potato. Physiol Mol Plant Pathol 41:61–72

Riggs RD (1988) Races of *Heterodera glycines*. Nematropica 18:163–170

Riggs RD (1992) Chapter 10: Host range. In: Riggs RD, Wrather JA (eds) Biology and management of the soybean cyst nematode. APS Press, St Paul, pp 107–114

Riggs RD, Schmitt DP (1988) Complete characterization of the race scheme for *Heterodera glycines*. J Nematol 20:392–395

Riggs RD, Schmitt DP (1991) Optimization of the *Heterodera glycines* race test procedure. J Nematol 23:149–154

Riggs RD, Kim KS, Gipson I (1973) Ultrastructural changes in Peking soybeans infected with *Heterodera glycines*. Phytopathology 63:76–84

Ross JP (1958) Host–Parasite relationship of the soybean cyst nematode in resistant soybean roots. Phytopathology 48:578–579

Ross JP (1962) Physiological strains of *Heterodera glycines*. Plant Dis Rep 46:766–769

Sardanelli S, Kenworthy WJ (1997) Soil moisture control and direct seeding for bioassay of *Heterodera glycines* on soybean. J Nematol 29(suppl):625–634

Sasai H, Ishida M, Murakami K, Tadokoro N, Ishihara A, Nishida R, Mori N (2009) Species-specific glucosylation of DIMBOA in larvae of the rice Armyworm. Biosci Biotechnol Biochem 73:1333–1338

Sass JE (1958) Botanical microtechnique. Iowa State College Press, Ames

Sasser JN, Freckman DW (1987) A world perspective on nematology: the role of the society. In: Veech JA, Dickerson DW (eds) Vistas on nematology. Society of Nematologists, Hyattsville, pp 7–14

Scheideler M, Schlaich NL, Fellenberg K, Beissbarth T, Hauser NC, Vingron M, Slusarenko AJ, Hoheisel JD (2002) Monitoring the switch from housekeeping to pathogen defense metabolism in *Arabidopsis thaliana* using cDNA arrays. J Biol Chem 277:10555–105561

Schmelzer E (2002) Cell polarization, a crucial process in fungal defence. Trends Plant Sci 7:411–415

Shannon JG, Arelli PR, Young LD (2004) Breeding for resistance and tolerance. In: Schmitt DP, Wrather JA, Riggs RD (eds) Biology and management of soybean cyst nematode, 2nd edn. Schmitt & Associates of Marceline, Marceline, pp 155–180

Sobolev VS, Neff SA, Gloer JB (2010) New dimeric stilbenoids from fungal-challenged peanut (*Arachis hypogaea*) seeds. J Agric Food Chem 58:875–881

The Gene Ontology Consortium (2004) The gene ontology (GO) database and informatics resource. Nucleic Acids Res 32:D258–D261

Tzafrir I, Pena-Muralla R, Dickerman A, Berg M, Rogers R, Hutchens S, Sweeney TC, McElver J, Aux G, Patton D, Meinke D (2001) Identification of genes required for embryo development in Arabidopsis. Plant Physiol 135:1206–1220

Wang Y, Cai QN, Zhang QW, Han Y (2006) Effect of the secondary substances from wheat on the growth and digestive physiology of cotton bollworm *Helicoverpa armigera* (Lepidoptera: Noctuidae). Eur J Entomol 103:255–258

Weyman PD, Pan Z, Feng Q, Gilchrist DG, Bostock RM (2006a) A circadian rhythm-regulated tomato gene is induced by Arachidonic acid and *Phytophthora infestans* infection. Plant Physiol 140:235–248

Weyman PD, Pan Z, Feng Q, Gilchrist DG, Bostock RM (2006b) DEA1, a circadian- and cold-regulated tomato gene, protects yeast cells from freezing death. Plant Mol Biol 62:547–559

Wrather JA, Koenning SR (2006) Estimates of disease effects on soybean yields in the United States 2003–2005. J Nematol 38:173–180

Wrather JA, Stienstra WC, Koenning SR (2001) Soybean disease loss estimates for the United States from 1996 to 1998. Can J Plant Pathol 23:122–131